The Open Civil Engineering Journal
DOI: 10.2174/0118741495500389261002114419, 2026, 20, e18741495500389
ISSN: 1874-1495
1

RESEARCH ARTICLE OPEN ACCESS

Experimental Investigation on Steel Fiber-reinforced Slag Aggregate Concrete: A Path Towards Green Construction

Maddula Rama Manikantha[1,*], Abdul Mateen Mohammed[1] and Sumit Choudhary[2]

[1]*Department of Civil Engineering, CMR University, Bengaluru, India*
[2]*Project Implementation Engineer, Systra MVA Consulting India Pvt. Ltd., Bengaluru, India*

Abstract:

Introduction/Objective: The depletion of natural aggregates and accumulation of steel slag waste pose environmental challenges. However, there is limited research on the combined effect of steel fiber and slag aggregate in concrete. This study evaluates the fresh, mechanical, durability, and microstructural properties of Steel Fiber-Reinforced Slag Aggregate Concrete (SFRSAC) to identify the optimum fiber content and slag replacement level for durable, sustainable concrete.

Methods: Twenty concrete mixes were prepared with varying amounts of steel fiber and slag aggregate replacing coarse aggregate. Fresh properties were assessed *via* the slump test, and hardened properties *via* compressive, flexural, and split tensile strength, ultrasonic pulse velocity, abrasion resistance, apparent density, permeable voids, water permeability, acid attack, and chloride penetration. The microstructure was investigated using detailed SEM analysis.

Results: Steel fiber improved mechanical performance, with the optimum mix achieving a compressive strength of 59 MPa, approximately 27% higher than conventional concrete. Slag aggregate enhanced acid and chloride resistance, and SEM confirmed a denser microstructure with improved interfacial bonding and reduced microcracking. Slag utilization reduced natural resource consumption and material cost.

Discussion: The interaction between steel fiber and slag aggregate improved mechanical properties, durability, and microstructural integrity, confirming that combining fiber reinforcement with industrial waste aggregate is an effective route to durable, high-performance, sustainable concrete.

Conclusion: Combined utilization of steel fiber and slag aggregate produces sustainable, high-performance concrete, with 3% steel fiber and 50% slag aggregate replacement giving the optimum overall performance. This mixture is recommended for structural and infrastructure applications requiring enhanced strength, durability, and sustainability.

Keywords: Steel fiber reinforced concrete (SFRC), Slag aggregate concrete (SAC), Mechanical properties, Durability performance, Sustainable construction materials, Infrastructural development.

© 2026 The Author(s). Published by Bentham Open.
This is an open access article distributed under the terms of the Creative Commons Attribution 4.0 International Public License (CC-BY 4.0), a copy of which is available at: https://creativecommons.org/licenses/by/4.0/legalcode. This license permits unrestricted use, distribution, and reproduction in any medium, provided the original author and source are credited.

* Address correspondence to this author at the Department of Civil Engineering, CMR University, Bengaluru, India; E-mail: rama.21cphd@cmr.edu.in

Cite as: Manikantha M, Mohammed A, Choudhary S. Experimental Investigation on Steel Fiber-reinforced Slag Aggregate Concrete: A Path Towards Green Construction. Open Civ Eng J, 2026; 20: e18741495500389.
http://dx.doi.org/10.2174/0118741495500389261002114419

Received: June 13, 2026
Revised: August 08, 2026
Accepted: August 18, 2026
Published: October 09, 2026

Send Orders for Reprints to reprints@benthamscience.net

1. INTRODUCTION

Concrete has been used at a very large scale in the infrastructural development of society over the last few decades due to its superior performance in compression. However, under tension, early failure has been observed. Therefore, fibers have been effectively used in the production of concrete to resist tensile loads [1]. Fibers can be of different types, including steel, rubber, glass,

and other natural or synthetic fibers. Extensive research has been carried out on the incorporation of these fibers as a replacement or additive in concrete. Also, the latest techniques and technologies are being used to prepare continuous fiber, which can even substitute for conventional reinforcement bars [2]. To attain better strength properties, FRCs are being used very extensively and at a high rate worldwide, including in India, for the construction of bridges, pavements, airports, and other high-strength concrete structures. Among the various fibers, steel fiber is predominantly used in concrete as a replacement or addition. Steel Fiber-Reinforced Concrete (SFRC) has consistently shown superior strength properties compared with Conventional Concrete (CC) [3, 4].

On the other hand, the use of natural raw materials is increasing owing to growing construction activity. This has resulted in the depletion of natural raw materials such as fine and coarse aggregates, and cement used for preparing concrete, as these materials are not abundant on Earth. Therefore, alternatives to these materials are being researched extensively for a sustainable and productive approach. To attain sustainability, it is necessary to use substitute materials that are more economical and have similar or better behavior than the basic raw materials. A large quantity of waste, such as slag, rubber, ceramic, and granite waste, is generated from various parent industries and is being dumped in landfills, while various other disposal methods are also being researched [5-7]. Slag is one such waste material produced in large quantities, most commonly obtained as a by-product of metal production in the steel and iron industries. Moreover, these wastes are hazardous to the environment and may cause serious health effects. The surface texture and size of slag aggregates are similar to those of the natural coarse aggregates used in concrete production. Hence, waste slag is being widely utilized by researchers and engineers as a substitute for coarse aggregates in the construction of engineering structures.

Many studies have been conducted on the application of steel slag aggregates in concrete. For example, in the United States, about 500–700 thousand tonnes of slag waste are reported to be used annually for engineering applications [8]. Several researchers [9, 10] have demonstrated the possibility of using slag waste in such applications as barrier layers, highways, cement production, hydraulic barriers, seaports, and landfill covers. Ibrahim *et al.* (2025) [11] showed that the use of steel slag as a fine aggregate improves the mechanical behavior of structural concrete while encouraging sustainable use of industrial waste; however, the combined effect of steel fiber and slag aggregates was not investigated in that study. In 2024 and 2025, Mitwally *et al.* [12] and Mohanta *et al.* [13] reported productive results from the use of slag aggregate in concrete. Li *et al.* (2023) [14] and Wei *et al.* (2024) [15] found that slag aggregates can replace fine and coarse aggregates in concrete by up to 50%.

Pal *et al.* (2025) [16] and Dutta and Singh (2023) [17] observed a reduction in workability values for slag aggregate concrete due to the porous structure and high absorption capacity of slag aggregates. Akhtar *et al.* (2025) [18] and Son *et al.* (2024) [19] reported improved mechanical properties of SAC, but the alterations in slag aggregate morphology and gradation led to increased water absorption and permeability.

Özcan *et al.* (2019) [20], Hu (2017) [21], and Li *et al.* (2024) [22] reported improvements in strength, resistance to chemical attack, and heat of hydration of slag-based concrete. In contrast, Gopalakrishnan and Nithiyanantham (2020) [23] reported only minor variation in the compressive strength of conventional and slag-based concretes, with a slight reduction in flexural strength. Chadee *et al.* (2025) [24] and Van Ho and Huynh (2023) [25] similarly confirmed improved strength with slag replacement of up to 35-50%. In contrast, some researchers reported a decrease in strength properties. Herki *et al.* (2025) [26] reported that strength decreased when mixed recycled and slag aggregates were used, but concrete containing only slag showed up to 67% improvement. According to Abdalla and Alahmari (2024) [27], the use of copper slag and silica fume improved compressive strength (10–15%) and split tensile strength (10–18%) owing to better bonding. Torres *et al.* (2017) [28], replacing 10–30% foundry slag, observed little change in strength and recommended its use in plain cement concrete (PCC). Singh *et al.* (2022) [29] reported that weathered LD steel slag aggregates showed improved mechanical and durability performance. Finally, Choudhary *et al.* (2022) [30] observed a reduction in strength when natural coarse aggregates were completely replaced with slag.

1.1. Research Significance

The existing literature shows that steel fiber has a strong ability to improve the tensile strength, ductility, crack resistance, and post-cracking behavior of concrete. Likewise, the application of steel slag as a sustainable substitute for natural coarse aggregates has been studied extensively. However, the reported mechanical and durability performance of slag aggregate concrete remains inconsistent due to significant variation in slag properties, replacement ratios, and aggregate characteristics adopted in previous investigations.

Many studies have been conducted on steel fiber-reinforced concrete and slag aggregate concrete separately, but very few have examined their combined effect on concrete performance. In particular, there is a lack of studies on the synergistic interaction between steel fiber and slag aggregates across a wide range of replacement levels, including complete (100%) replacement of natural coarse aggregate. Additionally, previous studies have mainly focused on mechanical properties, while comprehensive appraisals considering fresh properties, durability performance, microstructural features, sustainability indicators, and economic viability remain lacking.

To address these research gaps, the current study experimentally examines the combined use of hooked steel

fibers (0-3% by volume) and steel slag aggregates (0-100% replacement of 20 mm natural coarse aggregates) for the development of Steel Fiber Reinforced Slag Aggregate Concrete (SFRSAC). The steel fiber dosage range (0–3% by volume) is selected according to previous concrete study [1], which show a significant improvement in concrete strength and toughness in this range. At dosages higher than 3%, the workability decreased, and the tendency to form fiber balls increased. The levels of slag aggregate replacement (0–100%) were selected to facilitate a comprehensive assessment of the effect of partial and complete substitution of natural coarse aggregate, consistent with replacement ranges commonly reported in the literature [8, 25]. The proposed investigation is distinct from previous studies in that fresh properties, mechanical behavior, durability performance, SEM-based microstructural characteristics, embodied energy, embodied carbon emissions, and material cost are all evaluated simultaneously. In addition, the optimal combination of steel fiber dosage and slag aggregate replacement is identified to produce a sustainable, durable, and high-performance concrete suitable for structural applications.

The results offer a holistic understanding of the synergistic behavior of steel fiber and slag aggregates and contribute to the sustainable use of industrial by-products in concrete, thereby promoting resource conservation and environmentally friendly construction practices.

2. MATERIALS AND METHODS

2.1. Specification of Materials

In the present work, Ordinary Portland Cement (OPC) of grade 43, conforming to IS 8112:2013 [31] and having a specific gravity of 3.15, was used as the binding material. Natural crushed stone of basaltic origin, with a maximum nominal size of 10 mm and 20 mm, was used as Coarse Aggregate (CA), as shown in Fig. (**1a**). Fine Aggregate (FA) of zone II, with particle size passing a 4.75 mm sieve, was used. The aggregates were incorporated into the concrete in accordance with the codal provisions given in IS 383 [32].

A metal manufacturing byproduct (most commonly known as slag) procured from a nearby industry (Kakinada, Andhra Pradesh) has been used as a partial and complete replacement of 20 mm crushed natural coarse aggregates (Fig. **1b**). The Steel Fiber (SF) - hooked type, having an aspect ratio of 60 - was utilized in the study as an addition to the total volume of the concrete mix, and its sample is shown in Fig. (**2**). The grain size analysis for the natural coarse aggregates and waste slag coarse aggregates is performed further. Table **1** represents the basic physical properties of the cement, and Table **2** represents the raw aggregates and the slag aggregates. The specific gravity value for the coarse SA was slightly lower than that of natural aggregates.

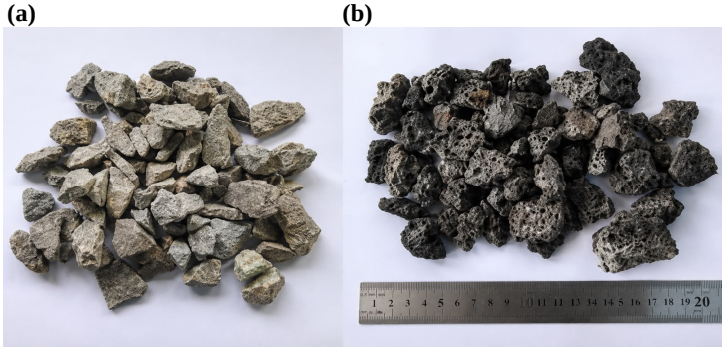

Fig. (1). Sample of (**a**) coarse aggregate and (**b**) slag aggregate.

Fig. (2). Sample of hook-type steel fiber.

Table 1. Physical properties of cement.

Physical Properties (units)	Consistency (%)	Initial Setting Time (mins)	Final Setting Time (mins)	Specific Gravity	Compressive Strength - 28 days (MPa)
Observed values	27	142	248	3.16	44.8

Table 2. Physical properties of natural aggregates and slag aggregates.

Properties	Fine Aggregates (FA)	Coarse Aggregates (CA)		Slag Aggregates (SA) 20 mm
		10 mm	20 mm	
Specific gravity	2.61	2.69	2.74	2.72
Water absorption (%)	0.2	0.9	0.9	7.5
Fineness Modulus	2.5	5.95	6.75	6.62

Table 3. Elemental composition of cement, natural aggregates, and waste slag aggregates.

Elements (Chemical Symbol)	Cement	Fine Aggregates (FA)	Coarse Aggregates (CA)	Slag Aggregates (SA)
Oxygen (O)	48.91	44.21	31.6	54.02
Calcium (Ca)	30.93	2.98	14.1	0.8
Silicon (Si)	12.07	26.87	47.8	21.34
Aluminum (Al)	3.88	9.27	0.8	5.1
Iron (Fe)	2.23	1.75	0.35	11.8
Magnesium (Mg)	0.58	0.17	9.5	0.9
Sodium (Na)	0.12	0.79	0.9	0.15
Potassium (K)	1.23	13.24	0.09	0
Sulfur (S)	0.05	0.47	1.4	1.2
LOI	3.97	-	-	-

SA exhibited a higher water absorption, up to 7.33 times that of natural CA. To account for this high water absorption, the slag aggregates were pre-soaked to a saturated surface-dry (SSD) condition, and the mixing water was adjusted before batching. The additional water absorbed by the slag aggregate was compensated for in the batch water quantity so that the effective water-to-cement ratio was maintained at 0.35 for all mixes; this ensured that the observed performance differences arose from the aggregate itself rather than from variation in effective water content. Energy-Dispersive X-Ray Analysis (EDX), also referred to as EDS or EDAX, was performed on the cement, fine aggregate, coarse aggregate, and slag aggregate (Table **3**), with higher peaks for an element indicating greater abundance. It can be observed from Table **3** that Calcium (Ca) was present in a higher proportion in cement, which may be responsible for its adhesive property. Compared with the natural coarse aggregate, SA showed an average silica content of 21.34%, against 47.8% for the natural coarse aggregate (Table **3**), which could explain the comparatively smaller reduction in strength observed for concrete containing slag aggregates. It can also be noted that considerable amounts of oxygen and silicon were present, which made the coarse SA suitable for use in concrete production.

SEM analysis was performed on the cement, fine aggregate, coarse aggregate, and waste coarse slag aggregate to examine the surface texture and particle size using a Nova NanoSEM 450 (Fig. **3a-d**).

The SEM images showed that the coarse SA had comparatively more voids than the natural CA, and that the surface texture of the FA was relatively smoother and harder. A shiny and smooth surface was observed in the SEM micrograph of the cement. A High-Range Water-Reducing Admixture (HRWA), “Master Glenium Ace 30,” was used in all concrete mixes to ensure proper flowability and stability. Normal potable water was used for mixing the concrete ingredients and for curing.

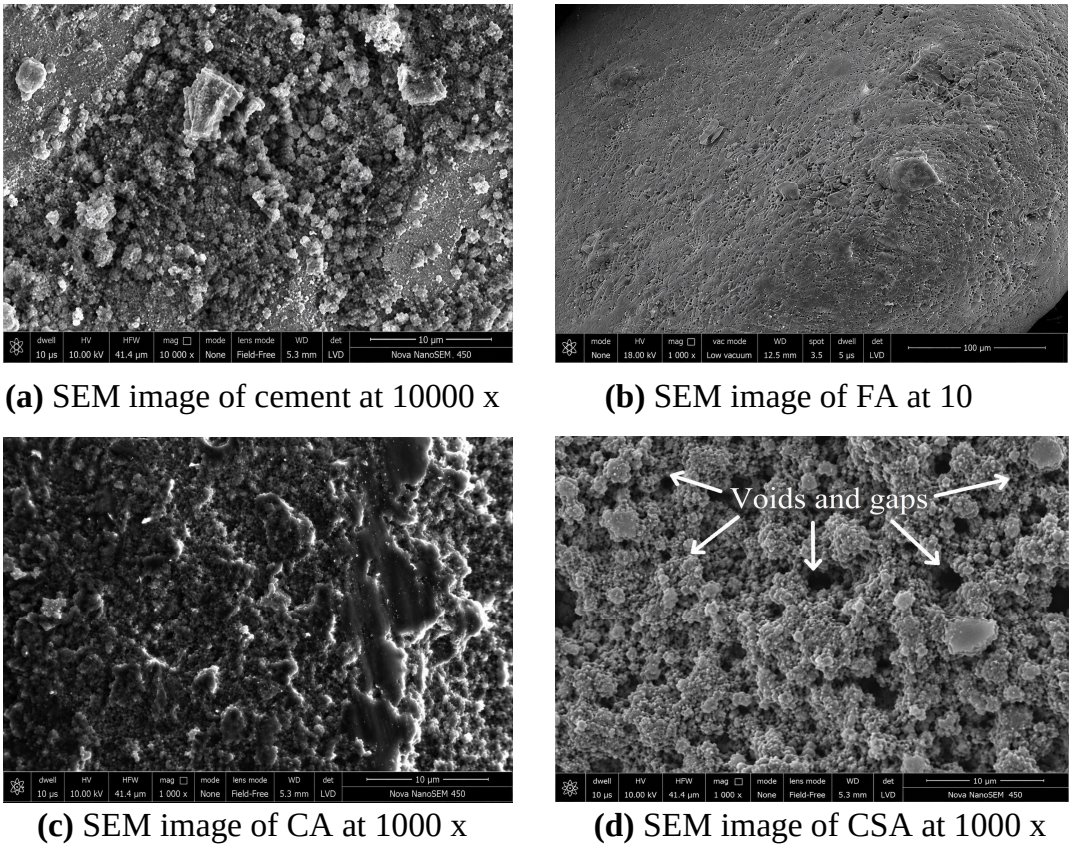

(a) SEM image of cement at 10000 x **(b)** SEM image of FA at 10

(c) SEM image of CA at 1000 x **(d)** SEM image of CSA at 1000 x

Fig. (3a-d). SEM images of materials.

2.2. Mix Design and Proportioning

In the present work, four different forms of concrete were cast: conventional concrete (CC), Steel Fiber Reinforced Concrete (SFRC), Slag Aggregate Concrete (SAC), and Steel Fiber Reinforced Slag Aggregate Concrete (SFRSAC). Steel fiber, at volumetric proportions of 0%, 1%, 2%, and 3% of the total mix volume, was added to produce SFRC. SAC was cast with partial and complete volumetric replacement of 20 mm coarse aggregate by coarse SA at 0%, 25%, 50%, 75%, and 100%. SFRSAC was cast with both SF and SA, added and replaced as described above. The w/c ratio was kept constant at 0.35 for all concrete forms. Hence, a total of 20 concrete mixes were prepared with and without SF and coarse SA, including the conventional concrete containing neither. The mix proportions for all concrete mixes are tabulated in Table **4**. Mix notations are in the form SFXSAY, where X denotes the Steel Fiber (SF) content (%), and Y denotes the steel slag (SA) content (%); SF0SA0 denotes the control or conventional concrete.

All raw materials used for the production of concrete were weighed according to the mix proportions and mixed in dry form (*i.e.*, without mixing water and HRWA) for 2 minutes in a rotating drum-type mixer. After dry mixing, two-thirds of the weighed water was added to the concrete mix and the mix was mixed for another 2 minutes. Finally, the remaining one-third of the water was added to the concrete mix along with the HRWA content, and the mixture was rotated for a further 4 minutes.

HRWA content was proportioned relative to the volume of cement in the concrete mix. The concrete mixture was removed from the mixer after mixing, and the fresh properties were investigated immediately. Thereafter, the concrete mixture was cast into pre-oiled iron molds, left to set for 24 ± 1 h to set, and then demoulded. The hardened concrete samples were cured in potable water for various durations before testing. Three concrete samples were cast for each mix.

2.3. Experimental Investigation Methodology

To ensure the repeatability and reliability of the experimental results, all concrete specimens were prepared using identical material proportions, mixing procedures, curing conditions, and testing protocols. For each concrete mix and each experimental test, three independent specimens were cast and tested in accordance with the respective Indian Standards and ASTM specifications. The reported results represent the average values of the three specimens. The observed variation among replicate specimens remained within the acceptable limits prescribed by the relevant standards, confirming satisfactory experimental repeatability.

Table 4. Mix quantities proportions (Kg/m^3).

-	Notation	Addition /Replacement	Cement	FA	CA		Water	SF	SA
					10 mm	20 mm			
Control concrete	SF_0SA_0	0%	400	600	300	900	140	0.00	0.00
Steel fiber (SF)	SF_1SA_0	1%	400	600	300	900	140	7.85	0.00
	SF_2SA_0	2%	400	600	300	900	140	15.70	0.00
	SF_3SA_0	3%	400	600	300	900	140	23.55	0.00
Slag Aggregates (SA)	SF_0SA_{25}	25%	400	600	300	675	140	0.00	225
	SF_0SA_{50}	50%	400	600	300	450	140	0.00	450
	SF_0SA_{75}	75%	400	600	300	225	140	0.00	675
	SF_0SA_{100}	100%	400	600	300	0	140	0.00	900
Steel fiber (SF) + Slag Aggregates (SA)	SF_1SA_{25}	1% + 25%	400	600	300	675	140	7.85	225
	SF_1SA_{50}	1% + 50%	400	600	300	450	140	7.85	450
	SF_1SA_{75}	1% + 75%	400	600	300	225	140	7.85	675
	SF_1SA_{100}	1% + 100%	400	600	300	0	140	7.85	900
	SF_2SA_{25}	2% + 25%	400	600	300	675	140	15.70	225
	$SF2SA_{50}$	2% + 50%	400	600	300	450	140	15.70	450
	SF_2SA_{75}	2% + 75%	400	600	300	225	140	15.70	675
	$SF2SA_{100}$	2% + 100%	400	600	300	0	140	15.70	900
	SF_3SA_{25}	3% + 25%	400	600	300	675	140	23.55	225
	SF_3SA_{50}	3% + 50%	400	600	300	450	140	23.55	450
	$SF3SA_{75}$	3% + 75%	400	600	300	225	140	23.55	675
	SF_3SA_{100}	3% + 100%	400	600	300	0	140	23.55	900

2.3.1. Fresh Concrete Test: Workability

To analyze the fresh properties of the concrete mix, workability was assessed using the slump test, performed as per the codal provisions in IS 1199 (2020) [33]. The fresh concrete was filled into an oiled conical mould in four approximately equal layers, each tamped by applying 25 strokes of a tamping rod. After pouring and tamping the final layer, the excess concrete was removed, and the mould was lifted slowly in the vertical direction. Finally, the slump was measured as the difference between the height of the mould and the height of the remaining concrete sample. The test was performed for each concrete mix containing SF, SA, or both.

2.3.2. Hardened Concrete Tests

2.3.2.1. Compressive Strength

The compressive strength of the concrete was evaluated after 28 and 90 days of curing using the provisions given in IS 516 (2021) [34]. A 150 mm cube was placed in a compression testing machine of 200-tonne capacity, and uniform loading was applied at a rate of 233.33 kN/m^2/s until failure occurred. The following formula was used to calculate the compressive strength of the cube (Eq. **1**):

$$\textbf{Compressive strength (N/mm}^2\textbf{ or MPa)} = P/A \quad (1)$$

where P = load applied (N) and A = area of the cube tested (mm^2)

2.3.2.2. Flexural Strength

Flexural strength was evaluated by testing beams of dimensions 500 × 100 × 100 mm as per the codal provisions in IS 516 (2021) [34]. The test was conducted on a universal testing machine using a three-point loading setup after 28 days of curing. The load was applied until failure at a loading rate of 30 N/s. To ensure accuracy, the test was performed on three samples from each mix, and the average value was taken as the flexural strength. The following formula was used to calculate the flexural strength (Eq. **2**):

$$\textbf{Flexural strength (N/mm}^2\textbf{ or MPa)} = 3PL/2bd^2 \quad (2)$$

where P = load applied (N), L = span length (mm), and b and d are the breadth (mm) and depth (mm) of the beam, respectively.

2.3.2.3. Split Tensile Strength

The splitting tensile strength test was performed to determine the bond strength of 150 mm × 300 mm cylindrical samples after 28 days of curing, according to the guidelines given in IS 516 (2021) [34]. The cylinders were placed between the loading platens of the compression testing machine, and the load was applied gradually until the sample failed by splitting. The split tensile strength was calculated using the following formula (Eq. **3**):

$$\textbf{Split tensile strength (N/mm}^2\textbf{ or MPa)} = 2P/\pi DL \quad (3)$$

where P = load applied (N), D = diameter (mm), L = span length (mm), and π = 3.14

2.3.2.4. Ultrasonic Pulse Velocity

To verify the integrity and quality of the concrete, the non-destructive Ultrasonic Pulse Velocity (UPV) technique

was used on 150 mm cubic specimens as per ASTM C597-22 (2022) [35]. To ensure proper contact, a sufficient amount of gel was applied to the concrete and the transducer surface, and the results are presented as pulse velocity to indicate the quality of the concrete.

2.3.3. Durability Test

2.3.3.1. Abrasion Resistance

The wear and abrasion resistance of the concrete samples was assessed by performing an abrasion test on 100 mm concrete cubes cured for 28 days, as per the procedure given in IS 1237 (2012) [36]. Three cubical specimens from each mix were oven-dried for 24 hours at a temperature of 110 ± 5 °C, and their weights were recorded before and after the test as W1 and W2, respectively. The oven-dried samples were fixed in a holding device mounted on a rotating platform and centrally loaded with a 300 N load. The platform was rotated at a speed of 30 rev/min, with 20 g of abrasive powder sprayed uniformly over 22 revolutions, after which the disc was stopped and the specimen rotated through an angle of 90° clockwise; the same procedure of 22 revolutions was then repeated nine times. The change in specimen thickness was evaluated using the following formula (Eq. **4**):

$$\text{Change in thickness (mm)} = (W_1 - W_2) \times V_1 / (W_1 \times A) \quad (4)$$

where W1 = initial mass of the specimen (g), W2 = final mass of the abraded specimen (g), V1 = initial volume of the specimen (mm^3), and A = surface area of the specimen (mm^2).

2.3.3.2. Apparent Density and Percentage of Permeable Voids

The apparent density and percentage of permeable voids in the concrete samples were evaluated to assess the durability of the concrete mix, as per the codal provisions in ASTM C642 [37]. The oven-dried cube samples were first weighed as W1, then kept in a boiling tank for 5-6 h and weighed again as W2. Finally, the weight of the cube immersed in water was recorded as W3. The apparent density (Eq. **5**) and percentage of permeable voids (Eq. **6**) were calculated as the mean of three samples using the following formulas:

$$\text{Apparent density (Kg/m}^3) = W_1 / (W_1 - W_3) \quad (5)$$

$$\text{Percentage content of permeable voids} = (W_2 - W_1) \times 100 / (W_2 - W_3) \quad (6)$$

where W1 = initial weight of the oven-dried cubes, W2 = weight of the cubes after boiling for 5-6 h, and W3 = weight of the water-immersed cubes.

2.3.3.3. Water Permeability

The water permeability test was conducted on 150-mm cubical specimens as per the provisions given in the German standard DIN 1048 [38]. A constant, uniform water pressure of 0.5 MPa was applied to the cubes for 72 hours (3 days), after which the cubes were removed and split in half. The depth of water ingress was then measured, in mm, using a scale. The permeability value for a concrete mix was calculated by averaging the penetration depths of three specimens.

2.3.3.4. Acid Attack

The effect of acid exposure on the concrete cubes was evaluated by conducting an acid attack test at 7, 28, and 56 days of exposure, in accordance with the guidance in ASTM C267-20 [39]. Oven-dried concrete cubes (100 mm) from each concrete mix were weighed (W1) and immersed in a 3% sulfuric acid (H2SO4) solution for different exposure durations. This 3% acid concentration was selected because it is widely adopted in accelerated durability studies and is consistent with ASTM C267 recommendations for evaluating the resistance of cementitious materials to aggressive acidic environments; it provides sufficiently severe exposure to assess degradation mechanisms within a practical laboratory testing period, while avoiding unrealistically harsh conditions that may not represent field exposure. The final weight (W2) was recorded after each exposure period, the percentage change in weight (Eq. **7**) was calculated, and the compressive strength (Eq. 1) of the respective cubes was also measured. The recorded compressive strength values were compared with those of the 28-day water-cured samples.

$$\text{Percentage change in weight (\%)} = (W_2 - W_1) \times 100 / W_2 \quad (7)$$

where W1 = initial oven-dried weight before acid exposure and W2 = final weight after acid exposure.

2.3.3.5. Chloride Penetration

The silver nitrate ($AgNO_3$) spray test was performed, following the method of Baroghel-Bouny *et al.* (2007) [40], to determine the chloride penetration depth. Concrete cube samples were immersed in a 3% NaCl solution for exposure periods of 28 and 90 days, after which the cubes were split into two parts. The split faces were then sprayed with a 0.1N $AgNO_3$ solution, and the penetration depth was measured based on the color change at the edge of the split faces. AgCl (white) is formed by the reaction of silver nitrate with chloride ions present in the hardened concrete matrix, whereas Ag_2O (dark brown) forms at greater depth by the reaction of silver nitrate with hydroxyl ions, as described in Eqs. (**8** and **9**).

$$Ag^+ + Cl^- \rightarrow AgCl \text{ (silver-white)} \quad (8)$$

$$Ag^+ + OH^- \rightarrow AgOH + Ag_2O \text{ (brown)} \quad (9)$$

3. RESULTS AND DISCUSSION

3.1. Fresh Property: Workability

The workability test was performed on the different control and modified concrete(s) to understand the placing and moving capability of the mix. Table **4** presents the HRWA content and slump values for each concrete mix with and without SF and SA. The comparison of workability for different mixes is presented in Fig. (**4**).

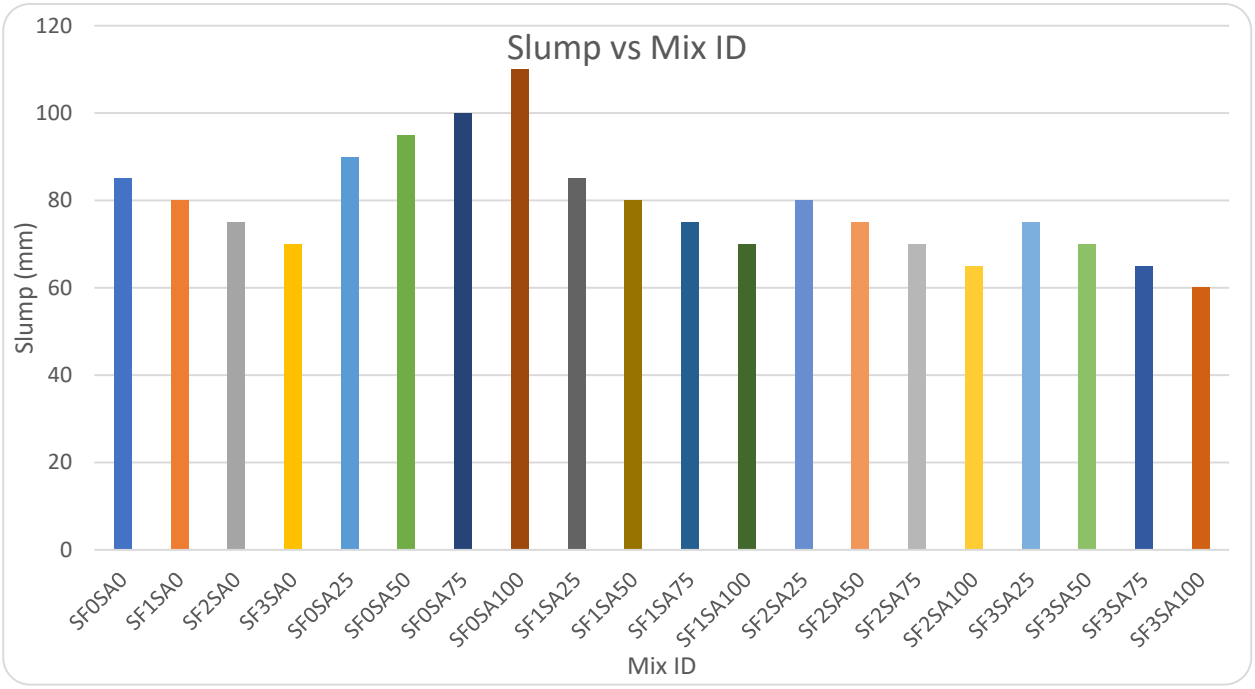

Fig. (4). Comparison of workability at different percentages of coarse aggregate replacement.

3.2. Hardened Properties

3.2.1. Compressive Strength

The compressive strength of all concrete mixtures at 28 and 90 days of curing is presented in Fig. (**5**). The results demonstrate that both Steel Fiber (SF) dosage and Slag Aggregate (SA) replacement ratio significantly influenced strength development, while their combined interaction governed the overall mechanical performance. As expected, all mixtures exhibited higher compressive strength at 90 days than at 28 days, indicating continued cement hydration and progressive refinement of the pore structure with curing age. The compressive strength varied from 38.0–51.0 MPa at 28 days and 44.0–59.0 MPa at 90 days.

The control concrete (SF0SA0) achieved compressive strengths of 40 MPa and 47.5 MPa at 28 and 90 days, respectively. Incorporation of steel fibers without slag aggregates progressively increased compressive strength to 45 MPa, 47.5 MPa, and 46 MPa at 28 days and 52 MPa, 55 MPa, and 53 MPa at 90 days for SF1SA0, SF2SA0, and SF3SA0, respectively. The maximum improvement was obtained with 2% steel fibers (SF2SA0), corresponding to an increase of approximately 18.8% at 28 days and 15.8% at 90 days compared with the control concrete. The improvement can be attributed to the crack-bridging action of steel fibers, which restricted the initiation and propagation of internal microcracks, thereby improving stress redistribution within the cement matrix. Similar observations have been reported by Yoo and Banthia (2016) [41] and ACI 544.1R [42], where steel fibers were shown to improve crack resistance, delay crack coalescence, and enhance compressive strength by increasing confinement within the matrix.

A slight reduction in strength was observed when the steel fiber content increased from 2% to 3%, although the strength remained higher than that of conventional concrete. The reduction is primarily associated with reduced workability caused by excessive fiber content, leading to fiber clustering (balling effect), entrapped air, and localized honeycombing during casting. These defects increase internal porosity and reduce matrix homogeneity, thereby limiting further strength development. Similar reductions in compressive strength beyond the optimum fiber dosage have been reported by Afroughsabet and Ozbakkaloglu (2015) [43].

The influence of slag aggregate replacement exhibited a different trend. When natural coarse aggregate was replaced with slag aggregate without steel fibers, the compressive strength remained comparable to conventional concrete up to 50% replacement. The highest compressive strength among the slag aggregate mixtures was recorded for SF0SA50, reaching 43.5 MPa at 28 days and 51.5 MPa at 90 days. The improvement observed at 50% replacement suggests that the rough, angular surface texture of slag aggregates enhanced mechanical interlocking with the cement paste, producing a relatively dense aggregate–paste interface. This finding is consistent with the improved aggregate interlock and comparable compressive strength typically reported for partial replacement of natural aggregates with steel slag aggregates.

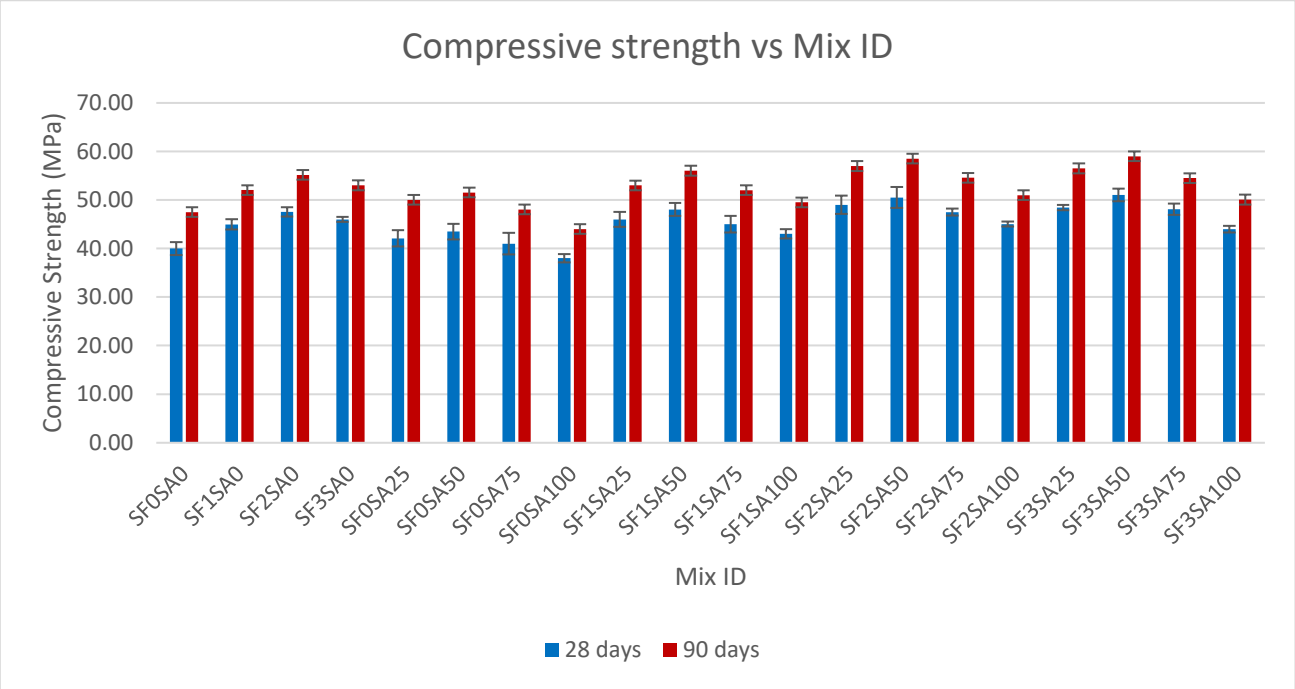

Fig. (5). Comparison of compressive strength at 28 days and 90 days for different percentages of coarse aggregate replacement.

However, increasing the slag aggregate replacement ratio to 75% and, particularly, to 100% resulted in a gradual reduction in compressive strength. The mixture SF0SA100 exhibited the lowest compressive strength (38 MPa at 28 days and 44 MPa at 90 days), representing approximately 7–8% lower strength than the control concrete. The reduction may be attributed to the relatively higher water absorption of slag aggregates, which increases internal moisture demand and promotes localized pores within the Interfacial Transition Zone (ITZ). Furthermore, the irregular pore structure and microvoids present within the slag aggregates reduce matrix continuity, creating weak regions that facilitate crack initiation under compressive loading. Similar reductions at higher replacement ratios have been attributed in the literature to excessive replacement of natural aggregates with industrial by-products, increasing ITZ porosity and reducing compressive strength.

A significantly different behavior was observed when steel fibers and slag aggregates were incorporated simultaneously. The hybrid concrete mixtures consistently exhibited higher compressive strength than the corresponding slag aggregate concrete without fibers, demonstrating the beneficial interaction between the two constituents. At 25% slag aggregate replacement, compressive strength increased from 46 MPa (SF1SA25) to 49 MPa (SF2SA25) and 48.5 MPa (SF3SA25) at 28 days, while the corresponding 90-day strengths reached 53 MPa, 57 MPa and 56.5 MPa, respectively. A similar trend was observed for 50% slag aggregate replacement, where compressive strength increased from 48 MPa (SF1SA50) to 50.5 MPa (SF2SA50) and further to 51 MPa (SF3SA50) at 28 days. At 90 days, the corresponding strengths increased to 56 MPa, 58.5 MPa and 59 MPa, respectively.

The superior performance of SF3SA50, which exhibited the highest compressive strength (59 MPa) among all mixtures, indicates that a 50% slag aggregate replacement provided an optimum aggregate skeleton while 3% steel fibers effectively confined the concrete matrix and restrained crack propagation. At this replacement level, the rough surface texture of slag aggregates promoted strong mechanical interlocking, whereas the fibers effectively redistributed internal stresses and delayed crack localization. The combined effect produced a dense and well-confined microstructure, consistent with the microstructural mechanisms discussed in Section 3.4, where the ITZ surrounding both slag aggregates and steel fibers appeared compact with limited microcracking.

However, when the slag aggregate replacement ratio increased beyond 50%, the beneficial contribution of steel fibers gradually diminished. Although the addition of steel fibers continued to improve compressive strength compared with the corresponding slag aggregate concrete, the improvement became less pronounced at 75% and 100% replacement. For example, the compressive strength of SF3SA75 decreased to 54 MPa, while SF3SA100 further decreased to 50 MPa after 90 days of curing. This indicates that excessive slag aggregate replacement increasingly controlled the failure mechanism by introducing higher porosity and weakening the aggregate–paste interface. Under these conditions, the

fibers continued to bridge developing cracks, but their effectiveness became dependent on the integrity of the surrounding cement matrix. Once the ITZ became more porous, stress transfer from the matrix to the fibers was reduced, limiting the overall strengthening effect.

A comparison between 28-day and 90-day strengths further demonstrates the influence of curing age on the modified concrete. All mixtures exhibited continued strength development between 28 and 90 days, with increases generally ranging from 7–9 MPa. The continued gain in strength indicates progressive hydration and further densification of the cement matrix and ITZ. The increase was particularly evident in mixtures containing both SF and SA, suggesting that the refined pore structure observed in the SEM analysis contributed to improved long-term strength development. Similar long-term strength enhancement in fiber-reinforced sustainable concrete has been attributed in the literature to ongoing hydration and progressive microstructural refinement.

Overall, the results demonstrate that the interaction between steel fiber dosage and slag aggregate replacement ratio governs compressive strength development rather than either constituent acting independently. Steel fibers effectively compensated for the reduction in strength associated with slag aggregate replacement by restricting crack propagation and improving stress redistribution, whereas slag aggregates contributed to enhanced mechanical interlocking up to 50% replacement. The optimum combination was achieved for SF3SA50, where 3% steel fiber and 50% slag aggregate replacement produced the highest compressive strength after 90 days of curing. Beyond 50% slag aggregate replacement, the increasing porosity and weaker ITZ gradually reduced the efficiency of fiber reinforcement, resulting in a decline in compressive strength despite continued crack-bridging action. These findings are in good agreement with recent investigations on steel fiber-reinforced sustainable concrete, which report that optimal mechanical performance is achieved through a balanced combination of fiber content and aggregate replacement rather than maximizing either parameter independently (Yoo and Banthia, 2016 [41]).

3.2.2. Flexural Strength

The flexural strength of all concrete mixtures after 28 days of curing is presented in Fig. (**6**). The results demonstrate that both Steel Fiber (SF) incorporation and Slag Aggregate (SA) replacement considerably influenced the flexural behavior of concrete, with the response governed by the interaction between fiber dosage and slag aggregate replacement level. The flexural strength ranged from 4.2 MPa to 7.4 MPa, indicating that the combined use of SF and SA can either enhance or reduce the tensile resistance depending on their proportions.

The control concrete (SF0SA0) exhibited a flexural strength of 5.2 MPa. Incorporation of steel fibers without slag aggregates progressively increased the flexural strength to 6.1 MPa (SF1SA0), 6.8 MPa (SF2SA0) and 6.4 MPa (SF3SA0), corresponding to improvements of approximately 17%, 31% and 23%, respectively. The optimum performance was achieved with 2% steel fiber, beyond which a slight reduction in strength was observed. This behavior indicates that an optimum fiber dosage exists for maximizing crack-bridging efficiency. At moderate fiber contents, steel fibers effectively arrest crack propagation, transfer tensile stresses across crack surfaces, and delay crack widening. However, excessive fiber dosage reduces workability and promotes fiber clustering, resulting in non-uniform distribution and localized voids that limit further strength enhancement (ACI 544.1R [42]).

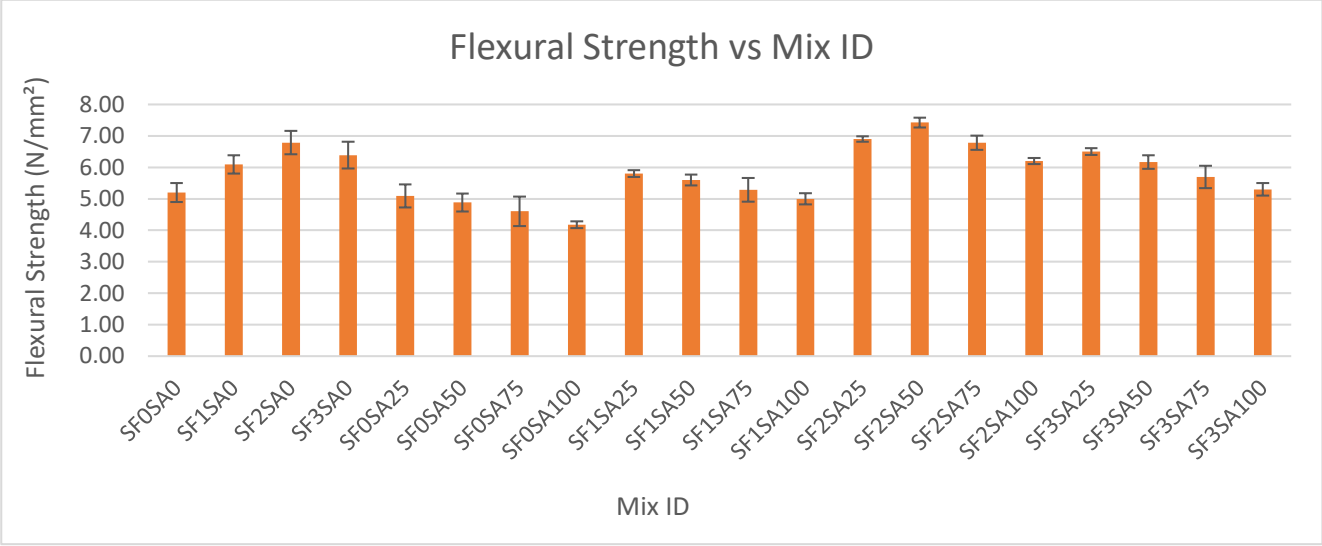

Fig. (6). Comparison of flexural strength for different percentages of coarse aggregate replacement.

The improvement in flexural strength can be attributed to the crack-bridging mechanism of hooked-end steel fibers. Under bending, microcracks initiate within the cement matrix, and the embedded fibers bridge these cracks, thereby transferring tensile stresses and increasing post-cracking load-carrying capacity. The hooked-end geometry with an aspect ratio of approximately 60 further enhances pull-out resistance through mechanical anchorage, thereby increasing fracture toughness and energy absorption. Similar mechanisms have been reported by Yoo and Banthia (2016) [41], who concluded that fiber orientation, aspect ratio, and bond characteristics primarily govern the flexural performance of steel fiber-reinforced concrete.

Unlike steel fibers, replacement of natural coarse aggregate with slag aggregate alone resulted in a gradual reduction in flexural strength from 5.1 MPa (SF0SA25) to 4.9 MPa (SF0SA50), 4.6 MPa (SF0SA75), and 4.2 MPa (SF0SA100). Although the reduction at 25% replacement was marginal, higher replacement levels significantly affected bending resistance. The decrease may be associated with the relatively higher water absorption and porosity of slag aggregates compared with natural crushed aggregates, which weaken the Interfacial Transition Zone (ITZ) and promote early crack initiation. Furthermore, the relatively brittle nature of slag particles limits their ability to redistribute tensile stresses under flexural loading. Similar reductions in flexural strength of slag aggregate concrete have been attributed in the literature primarily to increased pore volume and weaker aggregate–paste bonding.

A significantly different behavior was observed when steel fibers and slag aggregates were incorporated simultaneously. The inclusion of steel fibers effectively compensated for the reduction in flexural strength caused by slag aggregate replacement. At 25% slag replacement, flexural strength increased from 5.8 MPa (SF1SA25) to 6.9 MPa (SF2SA25) before slightly decreasing to 6.5 MPa (SF3SA25). Similarly, at 50% slag replacement, the strength increased from 5.6 MPa (SF1SA50) to a maximum value of 7.4 MPa (SF2SA50), then decreased to 6.1 MPa (SF3SA50). The SF2SA50 mixture exhibited approximately 42% higher flexural strength than conventional concrete, indicating a strong synergistic interaction between moderate slag aggregate replacement and optimum steel fiber dosage.

The superior performance of SF2SA50 suggests that moderate slag aggregate replacement improves aggregate interlocking while the steel fibers efficiently bridge developing cracks, resulting in improved tensile stress redistribution. The rough surface texture of slag aggregates may also enhance mechanical interlocking with the cement matrix, provided sufficient matrix integrity is maintained. Similar synergistic effects between recycled aggregates and steel fibers have been reported in the literature, in which an optimal fiber dosage effectively compensated for the reduction in tensile strength caused by the use of alternative aggregates.

However, the beneficial influence of steel fibers gradually diminished at higher slag aggregate replacement levels (75–100%). Although the addition of fiber still improved flexural strength compared with corresponding mixtures without fibers, the improvements became less significant. For example, flexural strength decreased from 6.8 MPa (SF2SA75) to 6.2 MPa (SF2SA100) despite maintaining the optimum fiber dosage. This indicates that excessive slag aggregate replacement increasingly governs the failure mechanism, thereby limiting the effectiveness of fiber reinforcement.

The reduced efficiency of fibers at higher slag contents can be explained by the combined effects of increased water absorption, higher internal porosity, weaker aggregate–paste bonding, and reduced workability. Simultaneous incorporation of high fiber volume and highly absorptive slag aggregates increases the probability of fiber balling, honeycombing, and uneven aggregate distribution, thereby reducing the crack-bridging efficiency of steel fibers. Similar observations have been reported in the literature, where excessive recycled or industrial aggregate replacement was found to weaken the matrix sufficiently to offset the benefits provided by fiber reinforcement.

Overall, the results clearly demonstrate that steel fiber dosage exerts a stronger influence on flexural performance than slag aggregate replacement, although the interaction between both materials is highly significant. Moderate slag aggregate replacement (25–50%) combined with an optimum steel fiber dosage (2%) produced the most favorable balance between sustainability and mechanical performance. In contrast, higher slag aggregate replacement (75–100%) reduced the effectiveness of fiber reinforcement because deterioration of matrix quality and interfacial bonding became the dominant controlling factors.

The relatively small error bars shown in Fig. (**6**) indicate good repeatability of the experimental results and confirm consistent specimen preparation and testing. Slightly higher variability observed for mixtures containing larger quantities of slag aggregates and steel fibers is attributed to local variations in fiber orientation, aggregate packing density, and interfacial transition zone characteristics, which is also consistent with observations reported by Yoo and Banthia (2016) [41].

3.2.3. Split Tensile Strength

The splitting tensile strength of the concrete mixtures cured for 28 days is presented in Fig. (**7**). The results demonstrate that both steel fiber incorporation and slag aggregate replacement substantially influenced the tensile performance of concrete. The tensile strength increased from 3.50 MPa for the control concrete (SF0SA0) to a maximum value of 5.75 MPa for the concrete containing 3% steel fiber and 100% slag aggregate replacement (SF3SA100), representing an overall enhancement of approximately 64.3% compared with the control mix. The observed improvement indicates a strong synergistic interaction between steel fibers and slag aggregate in resisting the propagation of tensile cracks.

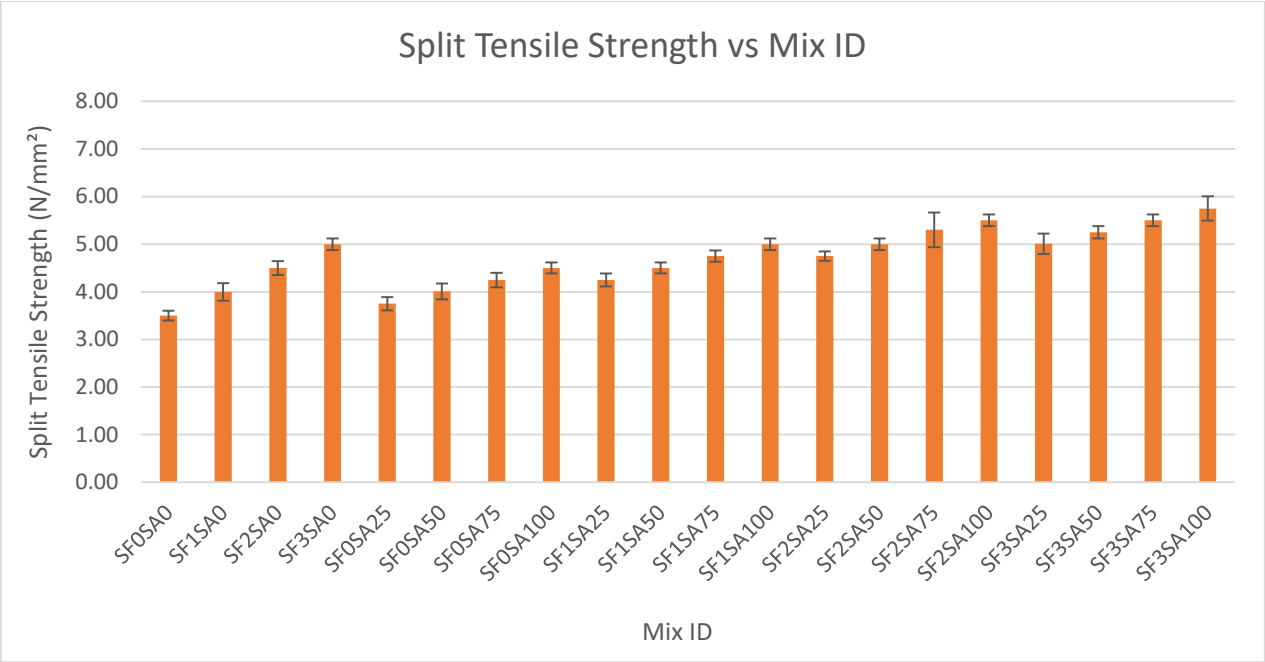

Fig. (7). Comparison of split tensile strength for different percentages of coarse aggregate replacement.

The influence of steel fiber content was considerably more pronounced than that of slag aggregate replacement alone. At a constant slag aggregate replacement level of 0%, increasing the steel fiber dosage from 0% to 3% increased the splitting tensile strength from 3.50 MPa to 5.00 MPa, corresponding to an improvement of approximately 42.9%. This enhancement can be attributed to the crack-bridging mechanism of steel fibers, which delays crack initiation and effectively transfers tensile stresses across developing cracks. The fibers act as discrete reinforcement, increasing fracture toughness and preventing sudden brittle failure. Consequently, fiber-reinforced mixtures exhibited a more ductile failure mode and retained load-carrying capacity even after matrix cracking.

Conversely, the incorporation of slag aggregate without steel fibers produced only moderate improvements. Increasing the slag aggregate replacement from 25% to 100% resulted in tensile strengths ranging from 3.75 MPa to 4.50 MPa, corresponding to improvements of approximately 7.1–28.6% over the control concrete. The gradual increase indicates that processed slag aggregate can effectively participate in load transfer through its rough and angular surface texture, which enhances the mechanical interlock at the aggregate–paste interface. Furthermore, the porous surface of slag particles promotes the deposition of hydration products around the aggregate, leading to a stronger Interfacial Transition Zone (ITZ). However, in the absence of steel fibers, the slag aggregate alone was insufficient to prevent unstable crack propagation after the peak tensile load, resulting in relatively brittle failure.

A more significant improvement was observed when steel fibers and slag aggregate were incorporated simultaneously, demonstrating a clear synergistic effect. For each fiber dosage, increasing the slag aggregate replacement consistently enhanced the tensile strength. For instance, mixtures containing 1% steel fiber exhibited an increase from 4.25 MPa at 25% slag replacement to 5.00 MPa at 100% replacement. Similarly, mixtures with 2% steel fiber increased from 4.75 MPa to 5.50 MPa, while those containing 3% steel fiber increased from 5.00 MPa to 5.75 MPa with increasing slag replacement. These results indicate that slag aggregate provides a stronger supporting matrix for effective stress transfer to the steel fibers, allowing the fibers to mobilize their crack-bridging capacity more efficiently.

The interaction between steel fibers and slag aggregate can be explained through microstructural mechanisms. Steel fibers arrest microcrack propagation by bridging cracks and redistributing tensile stresses over a larger volume of concrete. Simultaneously, the rough texture and higher surface irregularity of slag aggregates improve fiber anchorage and mechanical interlocking within the cement matrix. This stronger bond minimizes fiber pull-out and enables greater energy absorption before complete failure. Consequently, the combined use of steel fibers and slag aggregate significantly enhances both the peak tensile strength and the post-cracking load-carrying capacity.

The trend observed in Fig. (7) further indicates that the beneficial effect of slag aggregate becomes increasingly pronounced at higher fiber contents. At low fiber dosages (1%), the increase associated with slag replacement is relatively gradual, whereas at 3% steel fiber, the incremental improvement due to slag replacement becomes more substantial. This behavior suggests that an improved

aggregate skeleton enhances stress distribution around the fibers, thereby allowing greater utilization of fiber tensile resistance. Therefore, the improvement in tensile strength results not merely from the individual contribution of steel fibers or slag aggregate but from their combined interaction.

From the failure characteristics observed during testing, the control concrete and slag-aggregate concrete without fibers exhibited sudden splitting accompanied by rapid crack widening immediately after the peak load. In contrast, fiber-reinforced specimens remained intact even after visible cracking, as the fibers bridged the separated concrete halves and continued to transfer tensile stresses. Increasing the steel fiber content reduced crack width and delayed crack localization, indicating improved ductility and fracture resistance. Such behavior is particularly advantageous for structural elements subjected to repeated loading, impact loading, and seismic actions where crack control is critical.

The present findings agree well with previous investigations reported in the literature. Mastali and Dalvand (2016) [44] reported that increasing steel fiber volume fraction from 0.25% to 0.75% significantly enhanced the splitting tensile strength of self-compacting concrete owing to improved crack bridging and fiber–matrix interaction. Likewise, Zheng *et al.* (2018) [45] observed approximately 66.8% improvement in splitting tensile strength with 2% steel fiber, which closely corresponds to the maximum enhancement obtained in the present investigation (approximately 64%). Similar improvements have also been reported by Yazıcı *et al.* (2007) [46] and Afroughsabet and Ozbakkaloglu (2015) [43], who concluded that steel fibers substantially improve tensile strength, energy absorption capacity, and post-cracking behavior through effective crack arrest mechanisms. Furthermore, studies investigating steel slag aggregate as a natural aggregate replacement have consistently reported improvements in tensile strength due to enhanced aggregate interlock and a denser interfacial transition zone, supporting the trends observed in the present study.

Overall, the experimental results demonstrate that steel fiber content is the dominant factor controlling splitting tensile strength, whereas slag aggregate replacement acts as a complementary parameter that further enhances fiber efficiency by strengthening the aggregate–paste interface and improving stress transfer. Among all mixtures investigated, the SF3SA100 mixture exhibited the highest tensile strength, indicating that the combined incorporation of 3% steel fibers with 100% slag aggregate replacement provides the most effective balance between matrix strength, crack resistance, and post-cracking ductility.

3.2.4. Ultrasonic Pulse Velocity

UPV tests were performed on the samples with and without SF and SA for the 28 curing days. Pulse velocity results have been displayed in Fig. (**8**) for all the concrete mixes. The increase in the content of SF and SA has shown a mixed range. The mixture with an SF addition of 3% and SA replacement of 50% with natural aggregate has shown the highest pulse velocity value. This may be attributed to the improved binding properties of the newer materials and a denser structure of modified concrete. The improved performance was observed mostly for all the modified concrete containing SF.

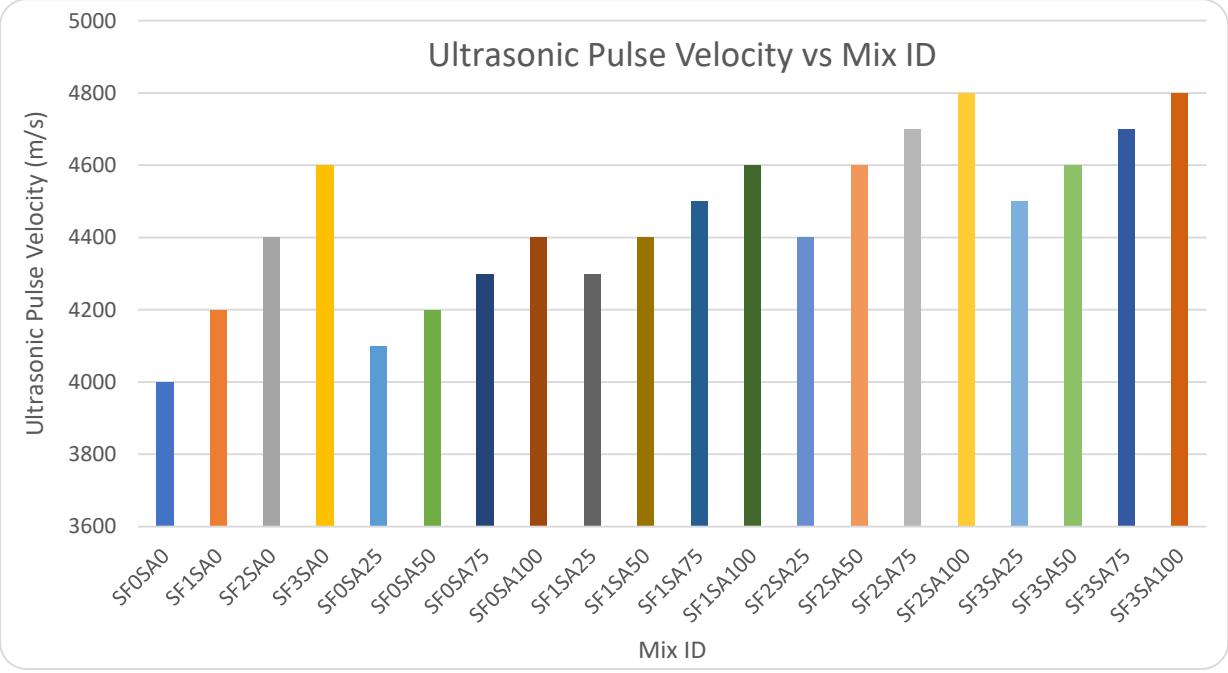

Fig. (8). Comparison of ultrasonic pulse velocity of concrete with different percentages of coarse aggregate replacement.

SF0SA0 (Plain Concrete, no fibers, no slag) serves as the reference mix. The addition of Steel Fiber (SF) improves the compactness and binding properties of the concrete, leading to higher pulse velocity. As the fiber content increases (SF1, SF2, SF3), the pulse velocity increases due to better structural integrity and fewer voids. SF3SA0 shows the highest UPV of 4600 m/s, indicating the highest density and compaction. Slag Aggregate (SA) replacement affects the UPV in a mixed manner. When combined with steel fiber, slag aggregates (25%, 50%, 75%, 100%) increase UPV due to improved packing and reduced void content. SF3SA50 has the highest UPV of 4600 m/s, showing the best performance when both steel fiber and slag aggregates are optimized.

SF3SA0 has the best performance among the mixes with only steel fiber (no slag replacement), which is likely due to better compaction and bonding properties. It exhibits the highest UPV of 4400 m/s. SAC mixes (slag aggregate content) typically show lower UPV values compared to fiber-reinforced mixes, as the porous and shiny surfaces of slag aggregates tend to absorb more of the pulse, leading to lower velocity values. Mixed SF and SA samples exhibit varying UPV values, with increased SF content improving the results due to the denser, stronger, and less porous structure. Similar trends have also been reported elsewhere [18].

3.3. Durability Properties

3.3.1. Abrasion Resistance

The wear-and-tear resistance of all the concrete samples was measured at 28 curing days by placing the oven-dried cube samples on the rotating disc of the abrasion machine. Figure **9** displays the wear-and-tear values for different modified concrete(s). The abrasion depth decreased with increasing SF and SA content. The highest abrasion resistance was observed for the conventional concrete, *i.e.*, SF0SA0. For the mixes containing only SF, wear and tear depth was found to increase with the increase in fiber content. The reason for this may be the hard, dense SF, which might have lost more of the surrounding concrete material during the wear and tear process. The depth of abrasion was found to be as high as 6.3 mm and as low as 5 mm for SF3SA0 and SF0SA0. Also, at a higher content of SF, the mix became heterogeneous, and a small number of voids and gaps led to a reduction in wear and tear resistance.

Samples containing only SA exhibited comparable performance to the Conventional Concrete (CC). The values for abrasion resistance were in the range of 5.10 mm to 5.4 mm for the concrete with and without slag. The depth of wear has shown an increasing trend for the samples with increasing SA content. The increase in the abraded depth for higher SA content can be due to the higher number of voids and gaps present in the aggregates and ultimately in the concrete mix. However, samples containing only SA performed better than those containing SF.

Mixes containing SF and SA both exhibited lower wear and tear resistance than conventional concrete. The minimum and maximum depths of wear and tear were found as 5.4 mm and 6.3 mm for SF1SA25 and SF3SA100, respectively. The higher abrasion depth was found due to the presence of hard and dense SF and comparatively porous SA.

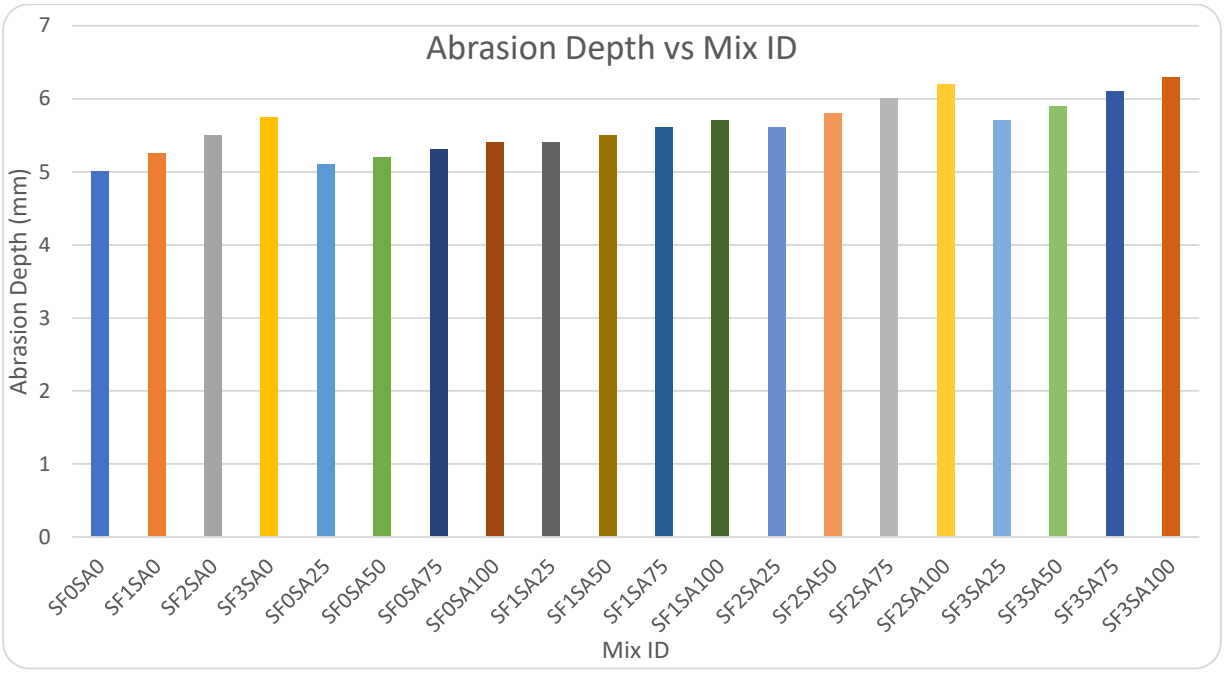

Fig. (9). Abrasion resistance of concrete with different percentages of coarse aggregate replacement.

SF0SA0 (Plain Concrete, no fibers, no slag) serves as the reference mix with an abrasion depth of 5.00 mm, which indicates the best wear and tear resistance. Mixes with SF only (SF1, SF2, SF3) show increasing abrasion depth as fiber content increases, which may be due to the hard, dense steel fiber causing the loss of surrounding concrete material. The higher the SF content, the more abrasion occurs, as fibers may lead to small voids and gaps in the mix. Mixes with only SA (slag aggregate) have shown slightly higher or comparable abrasion depths to those of conventional concrete. As SA content increases, the voids and gaps in the aggregates contribute to greater wear-and-tear resistance. Combined SF and SA mixes (*e.g.*, SF1SA50, SF2SA100) show increased wear and tear depth compared to conventional concrete due to the presence of both hard, dense fibers and the more porous slag aggregates. This combination results in weaker abrasion resistance.

3.3.2. Apparent Density and Percentage of Permeable Voids

The outcomes for the apparent density and percentage of permeable voids are displayed in Fig. (**10**). For the mixes containing SF and SA individually, an increase in density for the inclusion of SF and a decrease in the case of the addition of SA were observed. The maximum apparent density was observed for SF2SA0 and SF0SA25 for the SF and SA concrete mixes, respectively. The concrete mix without any SF and SA, *i.e.*, conventional concrete, showed an apparent density value of 2.3.

At the higher percentage of SF for both the series of mixes, with and without natural CA and waste SA, the density decreased comparatively. Illustrating, for the mix containing both SF and CA, the densities for SF2SA100 and SF3SA100 were 2.38 and 2.4, respectively. The higher proportion of SF in concrete may cause disturbance in the uniformity of the structure due to the balling effect and honeycombing [45, 47]. This balling effect ultimately results in large voids when the binding paste is not properly spread. The primary reason for honeycombing is insufficient and improper vibration.

The results indicate that the increase in density decreases the porosity or voids in the concrete. The formation of voids or gaps ultimately reduces the strength-bearing capacity and supports the fast deterioration of the concrete. The value for apparent density was slightly lower for the slag concrete as compared to other modified concrete due to light and less dense aggregates. A similar trend of results was observed for slag concrete by Choudhary *et al.* [30]. Figure **10** displays the relation between compressive strength and the percentage of permeable voids. It can be easily interpreted that with the rise in compressive strength, the percentage of permeable voids has automatically reduced.

3.3.3. Acid Attack

The attack on concrete samples by H_2SO_4 has been evaluated in terms of mass loss at various exposure periods and subsequent compressive strengths. The mechanism involved in the general deterioration of concrete due to acid attacks has been displayed in Fig. (**11**).

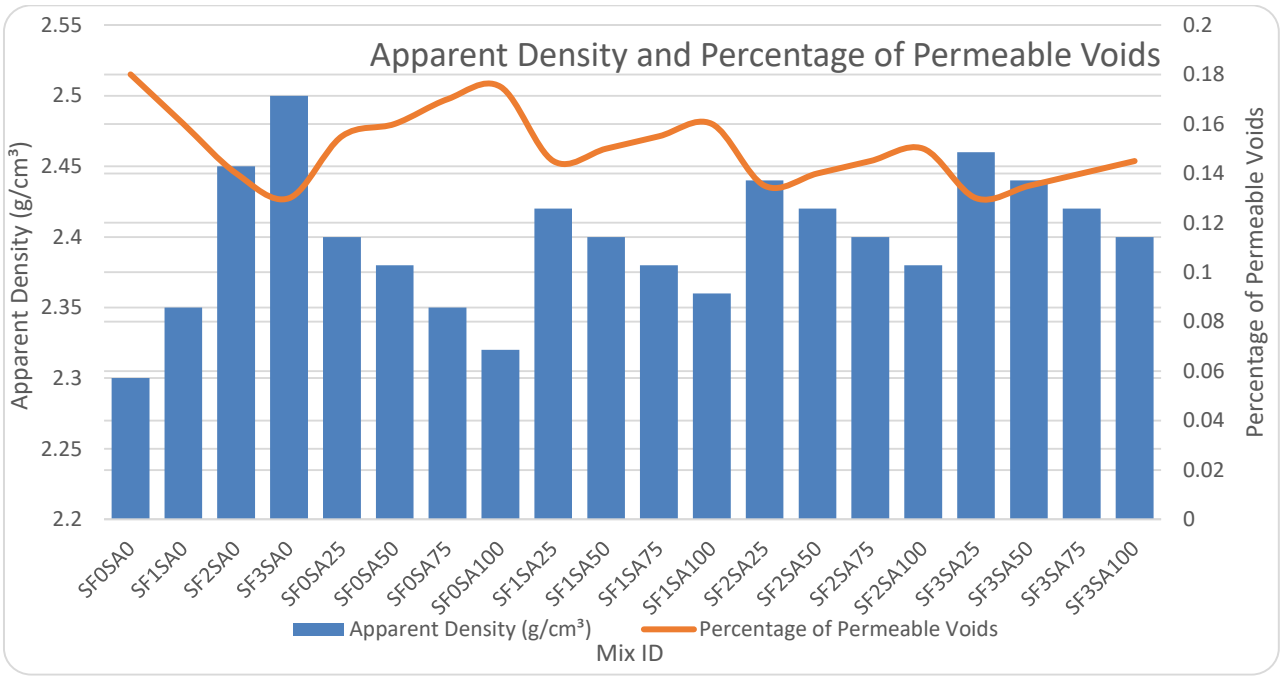

Fig. (10). Comparison of apparent density and percentage of permeable voids in concrete with different percentages of coarse aggregate replacement.

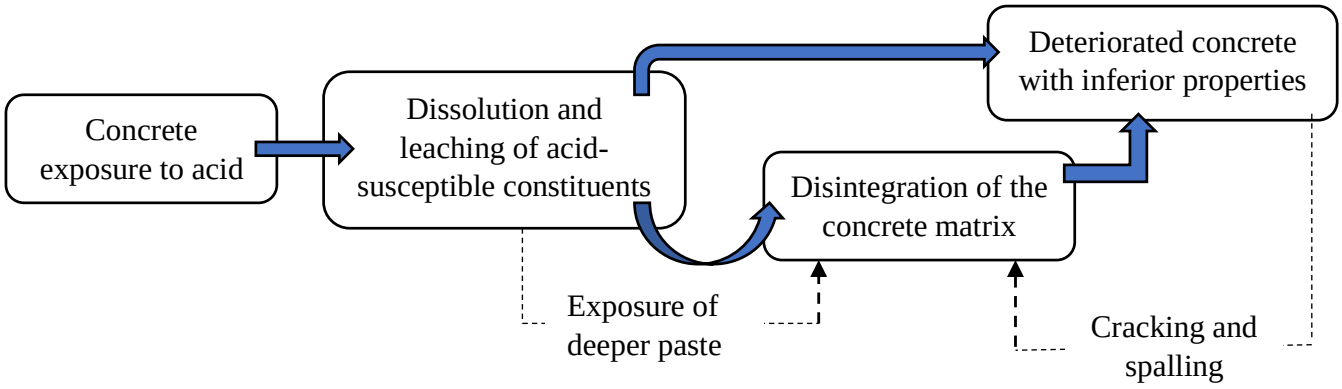

Fig. (11). Deterioration mechanism in concrete due to acid.

3.3.4. Visual Observations

The concrete cube samples exposed to 3% sulphuric acid (H_2SO_4) at various ages have shown the formation of gypsum on the upper layer. As shown in Fig. (**12**), the edges of the concrete deteriorated increasingly with the increase in exposure period for all forms of concrete. When sulphuric acid reacts with the calcium hydroxide present in concrete, gypsum is formed [48].

3.3.5. Mass Loss

The percentage reduction in mass due to deterioration of concrete has been shown in Fig. (**13**). The change in weight of concrete specimens has been calculated up to 90 days of exposure. The samples with SF in the mix initially showed a lower percentage of loss in mass, but with an increase in the SF content and exposure period, the deterioration increased. At the lower content of SF, deterioration was less due to the highly dense fiber structure. The increase in the SF percentage created more voids and gaps due to blockages by fibers, which ultimately induced more acid to penetrate and deteriorate. Also, samples in an acidic medium for a long duration of time deteriorated more. Samples with SA reacted comparatively better than the samples with or without SF. This can be due to the slag aggregate being less responsive to chemicals. However, with an increase in the exposure period, an increase in the mass loss was observed; for example, the percentage weight loss for 75% SA for 28 days' exposure was 2.3%, whereas at 90 days' exposure it was 4.9%. Samples with various proportions of SF and SA together performed better than the sample without SF and SA. As per the aforesaid statement, the sample with SF2SA50 had a percentage decrease in mass of 2.9%, whereas SF0SA0 showed a percentage loss of 4%.

Fig. (12). Visual observation of concrete exposed to acid attack.

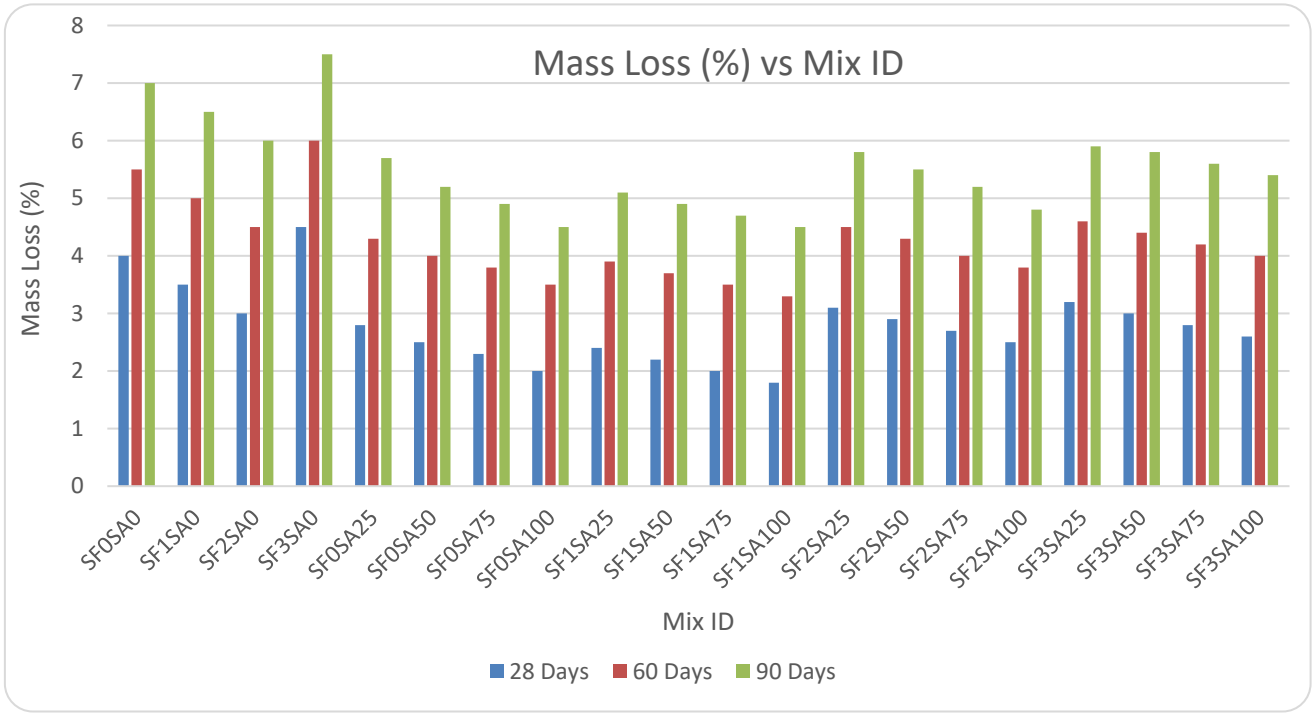

Fig. (13). Comparison of mass loss of concrete at 28, 60, and 90 days of curing under acidic exposure for different percentages of coarse aggregate replacement.

3.3.6. Loss in Compressive Strength

The value for the change in compressive strength has been represented graphically in Fig. (**14**). For all the modified concrete mixes, a greater decline in compressive strength was observed with an increase in the exposure period. During the initial days of exposure to the acidic medium, the decline was less, maybe due to the ettringite, which acted as a filler in the concrete. The samples across all concrete mixtures showed a loss in compressive strength of 6%, 8.5%, and 11% for SF0SA0 for 28, 60, and 90 days, respectively. The loss in compressive strength of concrete was higher in the case of samples having natural crushed aggregates. This might be due to the depolymerization of hydration products (CSH (calcium silicate hydrate) and CASH (calcium aluminate silicate hydrate)). The upper layer of the acid-attacked samples showed some pulp formation, which may result in the initiation of early cracks and the wearing away of surface layers.

For the acidic exposure up to 90 days, the deteriorated cubes showed a fall in compressive strength by 9.5%, 8.5%, 8%, and 11% for SF2SA0, SF0SA50, SF2SA50, and SF0SA0, respectively. Lower degradation has been observed for the samples containing SF and SA, individually as well as together. The reason for this could be improved bonding action between the foreign materials and the concrete constituents. This phenomenon of binding restricts cracking and material estrangement of concrete.

3.4. Microstructural Analysis

3.4.1. Sample Preparation for SEM Analysis

Scanning Electron Microscopy (SEM) was utilized to examine the microstructural characteristics of the various concrete mixes, including Conventional Concrete (CC), Steel Fiber Reinforced Concrete (SFRC), Slag Aggregate Concrete (SAC), and Steel Fiber Reinforced Slag Aggregate Concrete (SFRSAC). The objective of the SEM analysis was to identify morphological differences, bonding characteristics, and the influence of Steel Fiber (SF) and Slag Aggregates (SA) on the microstructure and Interfacial Transition Zone (ITZ) in the concrete.

Concrete samples were collected from the hardened specimens after curing for 28 days. Small fragments (10–15 mm) were extracted from the interior of the samples to avoid surface contamination. The fragments were dried at 60°C for 24 hours to eliminate moisture content. Following drying, the samples were coated with a thin layer of gold using a sputter-coating machine to enhance conductivity during SEM imaging.

3.4.2. Observations of SEM Analysis

3.4.2.1. Conventional Concrete (CC)-SF0SA0

The microstructure of conventional concrete exhibited a relatively porous ITZ, with visible microcracks and a moderate level of calcium hydroxide crystals. The matrix-aggregate bond appeared weaker compared to modified concrete mixes due to the absence of steel fiber or slag aggregates.

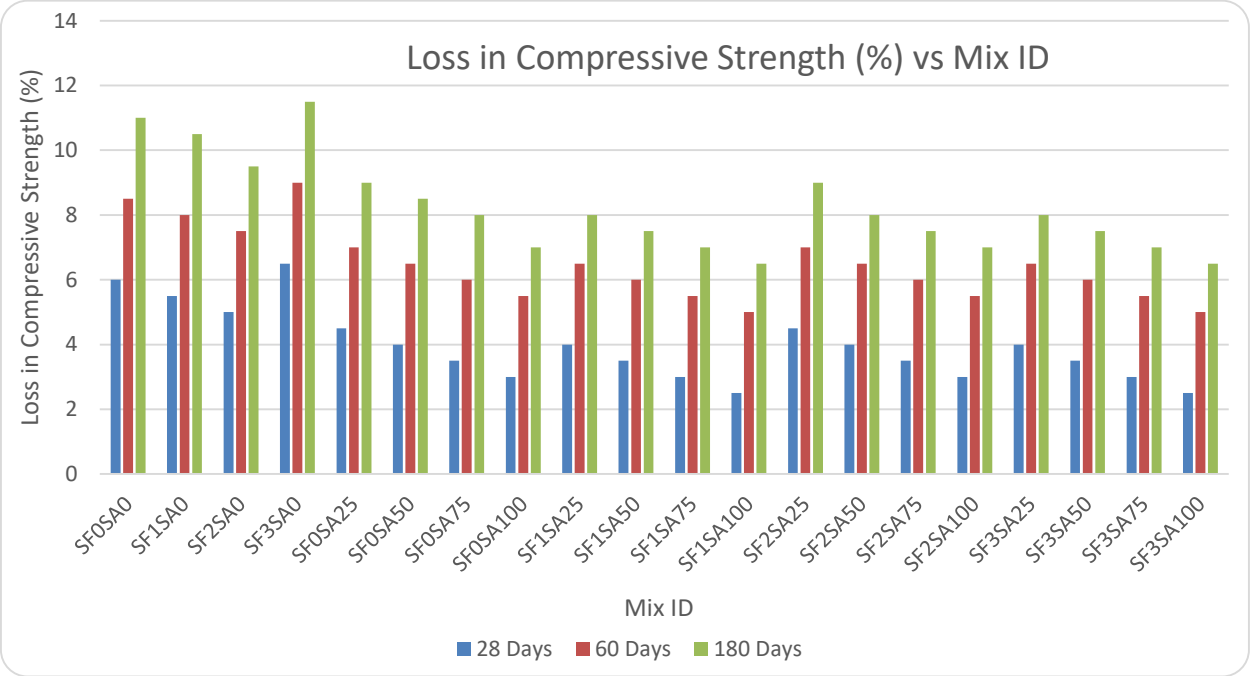

Fig. (14). Comparison of loss of compressive strength of concrete at 28, 60, and 90 days of curing under acidic exposure for different percentages of coarse aggregate replacement.

3.4.2.2. Steel Fiber Reinforced Concrete (SFRC)

SEM analysis revealed improved microstructural densification in the ITZ around the steel fiber. The incorporation of steel fiber at higher volumetric proportions (2% and 3%) contributed to reduced porosity and better crack-bridging capabilities. Steel fiber exhibited strong adhesion to the cementitious matrix, thereby enhancing mechanical interlocking.

3.4.2.3. Slag Aggregate Concrete (SAC)

The replacement of natural aggregates with slag aggregates altered the microstructure significantly. SAC with 50% and 75% slag aggregates showed a denser ITZ due to the pozzolanic reaction of slag, which reduced calcium hydroxide content and contributed to the formation of secondary calcium silicate hydrate (C-S-H) gels, which is consistent with the observations reported in [18] and by Li *et al.* (2024) [22]. Complete replacement (100%) of natural aggregates with slag aggregates resulted in minor segregation in some samples, which could marginally affect uniformity.

3.4.2.4. Steel Fiber Reinforced Slag Aggregate Concrete (SFRSAC)

The SEM micrographs presented in Figs. (**15** and **16**) provide clear evidence of the influence of Steel Fiber (SF) content and slag aggregate (SA) replacement on the pore structure and Interfacial Transition Zone (ITZ) of the concrete matrix. The microstructural observations correlate well with the mechanical performance, particularly the compressive and flexural strength results, indicating that the interaction between SF and SA governs the development of a denser and more stable cementitious matrix.

The microstructure of the Control Concrete (CC) (Fig. **15a**) exhibits a comparatively porous matrix with discontinuous hydration products and several microvoids within the ITZ. The transition zone surrounding the aggregate particles appears relatively weak due to loosely packed hydration products and localized pores, providing preferential paths for crack initiation and propagation under loading. Such a porous ITZ is generally recognized as the weakest region in conventional concrete, where tensile stresses concentrate during crack formation.

With the incorporation of steel fibers, the microstructure becomes noticeably denser (Fig. **15b**). The fiber–matrix interface shows improved bonding, and the hydration products are more uniformly distributed around the embedded fibers. The steel fibers serve as physical restraints against crack opening, resulting in fewer and narrower microcracks within the surrounding paste. Instead of allowing cracks to propagate freely through the matrix, the fibers bridge developing cracks and redistribute tensile stresses into the adjacent cement paste. Consequently, the ITZ surrounding the steel fibers appears more compact than that of the control concrete, indicating improved stress transfer between the cement matrix and the reinforcement.

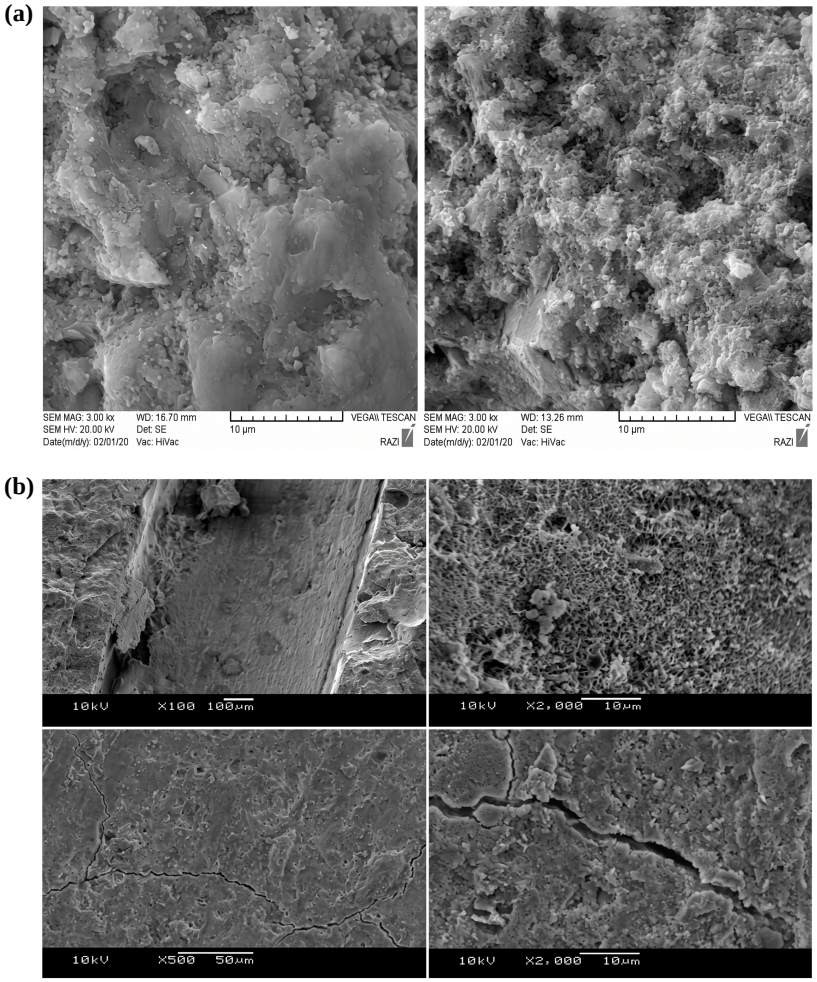

Fig. (15). SEM images of the (**a**) Control Concrete, (**b**) SF Concrete.

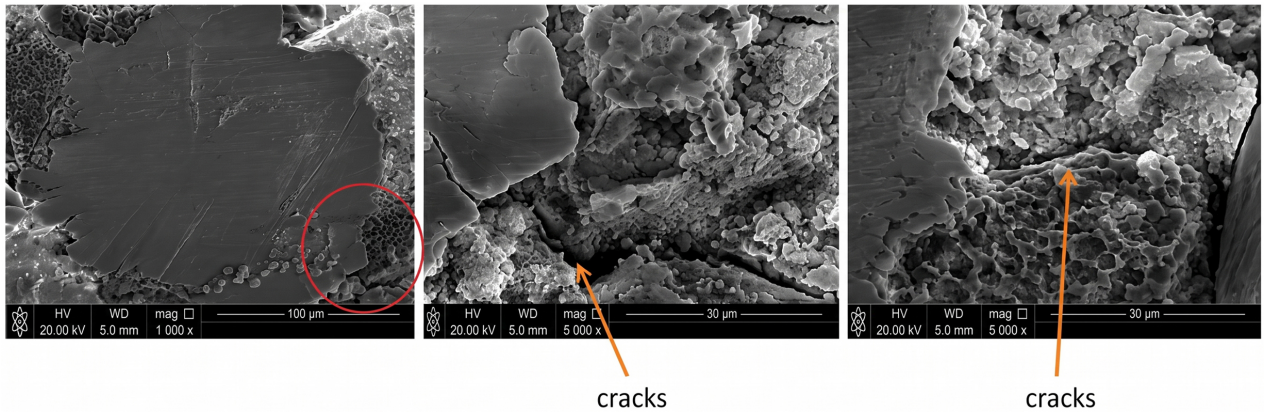

Fig. (16). SEM images of the combined effect.

The influence of slag aggregate replacement is particularly evident in the morphology of the ITZ. At moderate replacement levels, the ITZ surrounding slag aggregates appears denser than that of conventional concrete, with fewer interconnected pores and a more continuous network of hydration products. The rough and angular surface texture of slag aggregates enhances mechanical interlocking with the cement paste, thereby reducing the thickness of the weak transition zone. Furthermore, the presence of finer hydration products

within the ITZ indicates that the interfacial region becomes progressively refined, leading to improved bond characteristics between the aggregate and cement matrix.

The interaction between steel fibers and slag aggregates produces a synergistic refinement of the concrete microstructure. As shown in Fig. (**16**), hydration products densely surround both the steel fiber surface and the adjacent slag aggregate particles, leaving very limited interfacial gaps. The combined action of the rough slag aggregate surface and fiber reinforcement promotes the formation of a continuous, compact ITZ, reducing the connectivity of capillary pores. This refined microstructure provides a stronger load-transfer mechanism between aggregates, fibers, and the cement matrix, explaining the enhanced compressive and flexural strengths observed experimentally.

The SEM images also demonstrate the influence of SF and SA on the evolution of pore structure. The control concrete contains relatively larger pores and discontinuous void networks, whereas the modified mixtures exhibit a finer and less connected pore system. Steel fibers do not directly reduce porosity through chemical reactions; instead, they limit crack growth and restrict the enlargement of pores generated during loading. Simultaneously, the slag aggregate contributes to a more compact packing of the matrix at moderate replacement levels, reducing interparticle voids around the aggregate surface. The combined effect is a reduction in pore connectivity rather than merely a reduction in total pore volume, which is particularly beneficial for mechanical performance.

The crack morphology shown in Fig. (**16**) further illustrates the beneficial interaction between SF and SA. The observed cracks are relatively narrow and tend to terminate or deviate when approaching the steel fiber interface, indicating efficient crack-bridging action. Crack propagation is interrupted because the embedded fibers transfer tensile stresses across the crack surfaces, increasing the energy required for further crack growth. Around the slag aggregate particles, the cracks remain confined within the cement matrix rather than extending along the aggregate–paste interface, suggesting improved interfacial bonding and a stronger ITZ.

However, the beneficial microstructural effects are expected to diminish as the slag aggregate replacement ratio becomes excessively high. At higher replacement levels, the increased water absorption of slag aggregates and the greater demand for paste can lead to localized porosity and a less homogeneous ITZ. Although steel fibers continue to bridge developing cracks, their effectiveness becomes dependent on the integrity of the surrounding matrix. Where the ITZ contains larger pores or weak bonding, the stresses transferred by the fibers cannot be fully sustained, reducing the efficiency of crack arrest and limiting further improvements in mechanical performance. This observation is consistent with the slight reduction in compressive and flexural strength observed for mixtures containing the highest slag aggregate replacement levels.

Overall, the SEM observations demonstrate that the interaction between approximately 2% steel fiber content and slag aggregate replacement (SF2SA50) produces the most refined pore structure and the densest ITZ. The compact fiber–matrix interface, reduced pore connectivity, and improved aggregate–paste bonding collectively enhance crack resistance and load transfer, thereby providing the microstructural basis for the superior mechanical performance observed in the experimental investigation. These observations are consistent with previous studies reporting that steel fibers improve crack-bridging capability while slag aggregates refine the aggregate–paste interface, resulting in a denser and more durable concrete microstructure [18, 22].

CONCLUSION

The present study successfully explored the potential of Steel Fiber Reinforced Slag Aggregate Concrete (SFRSAC) as a sustainable and high-performance construction material. A comprehensive investigation into the mechanical, durability, and microstructural properties was carried out by varying the proportions of steel fiber (0–3%) and slag aggregates (0–100%). The key findings can be summarized as follows:

- Mechanical Performance: The incorporation of steel fiber significantly enhanced the compressive, flexural, and split tensile strength of concrete. Optimal performance was observed for the mix with 3% SF and 50% SA (SF3SA50), showing up to a 27% increase in compressive strength over conventional concrete. Excessive fiber content beyond 2%–3% led to a minor strength reduction due to balling and void formation.
- Durability Properties: While slag aggregates slightly reduced workability and abrasion resistance due to their porous texture, their use improved acid resistance and chloride penetration performance. The combined use of SF and SA led to reduced mass loss and strength degradation under acid attack, demonstrating better long-term durability.
- Microstructural Enhancement: SEM analysis suggests improved Interfacial Transition Zones (ITZs), denser microstructure, and reduced microcracks in SFRSAC mixes. Steel fibers contributed to crack bridging, while slag aggregates promoted secondary C-S-H formation through pozzolanic action. Similar observations have been reported in [18] and by Li *et al.* (2024) [22].
- Sustainability Aspects: The substitution of natural coarse aggregates with industrial waste slag and the use of minimal steel fiber lead to a reduction in embodied energy, a reduction in CO_2 emissions, and cost-effective concrete solutions. A quantified investigation of sustainability parameters can be considered the future scope of this work.

Although individual performance indices favored slightly different mix proportions, the overall optimum mix (SF3SA50) was identified by jointly considering fresh properties, mechanical strength, durability, and microstructural quality. This mix provided the most

balanced combination of properties without significantly compromising any individual performance criterion, making it the most suitable composition for structural applications. In conclusion, SFRSAC has shown considerable potential for structural and infrastructure applications, especially where sustainability, durability, and strength are critical.

STUDY LIMITATIONS

The synergy of steel fiber and slag aggregates proves beneficial in enhancing performance without compromising eco-efficiency. However, the study also highlights some of the limitations observed in the present study as listed below,

Firstly, the present experimental study is conducted entirely in a laboratory environment with concrete cube specimens. Therefore, its implementation at real-world scale under varying environmental conditions requires full-scale testing of structural members such as beams, columns, and slabs.

Secondly, the slag aggregates used in this work are considered only from a single source. The behavior of the aggregate may vary significantly if sourced from other places. It is therefore necessary to verify the behavioral changes of concrete for material sourced from multiple regions before its potential use in structures.

Thirdly, the durability study does not explore the behavior of concrete under cyclic loading, freeze–thaw conditions, creep, shrinkage, and fatigue.

Along with quantitative analysis, a quantitative characterization reveals the behavior of concrete more reliably. Therefore, techniques such as X-ray Diffraction (XRD), Thermogravimetric Analysis (TGA), or Mercury Intrusion Porosimetry (MIP) need to be implemented to facilitate understanding of hydration products and pore structure evolution of final products.

FUTURE SCOPE

Future research may focus on real-time field validation and long-term monitoring of SFRSAC structures to support wider practical implementation. A comprehensive life cycle and service life assessment of SFRSAC also needs to be evaluated to understand the degree of suitability of the product. The applicability of advanced data-driven techniques can also be investigated further for predicting the characteristics of such concrete to avoid time-consuming and cost-intensive experimental investigations.

AUTHORS' CONTRIBUTIONS

The authors confirm their contributions to the paper as follows: M.R.M and A.M.M: Study conception and design; M.R.M.: Data collection; A.M.M, M.R.M, and S.C.: Analysis and interpretation of results; M.R.M and S.C.: Draft manuscript. All authors reviewed the results and approved the final version of the manuscript under the Heading of Author Contribution.

LIST OF ABBREVIATIONS

SFRSAC	=	Steel fiber reinforced slag aggregate concrete
SAC	=	Slag aggregate concrete
SFRC	=	Steel fiber reinforced concrete
SF	=	Steel fiber
SA	=	Slag aggregate
CA	=	Coarse aggregate
HRWA	=	High range water admixture
SEM	=	Scanning electron microscopy
EDSX	=	Energy-dispersive X-ray analysis

CONSENT FOR PUBLICATION

Not applicable.

AVAILABILITY OF DATA AND MATERIALS

The data supporting the findings of this article are not currently deposited in a public repository. The data generated and/or analyzed during the current study will be made available from the corresponding author [M.R.M] upon reasonable request.

FUNDING

None.

CONFLICT OF INTEREST

The authors declare no conflict of interest, financial or otherwise.

ACKNOWLEDGEMENTS

The authors gratefully acknowledge the Material Research Center, MNIT Jaipur, India for carrying out SEM analysis.

REFERENCES

[1] S. Lolla, R.M. Oinam, A. Furtado, and H. Varum, "Tensile strength and flexural behavior of steel fiber-reinforced concrete beams", *Struct. Concr.,* vol. 26, no. 1, pp. 501-530, 2025. [http://dx.doi.org/10.1002/suco.202400074]

[2] R.B. Ramesh, O. Mirza, and W.H. Kang, "Mechanical properties of steel fiber reinforced recycled aggregate concrete", *Struct. Concr.,* vol. 20, no. 2, pp. 745-755, 2019. [http://dx.doi.org/10.1002/suco.201800156]

[3] T.M. Pham, "Fibre-reinforced concrete: State-of-the-Art-review on bridging mechanism, mechanical properties, durability, and eco-economic analysis", *Case Stud. Constr. Mater.,* vol. 22, p. e04574, 2025. [http://dx.doi.org/10.1016/j.cscm.2025.e04574]

[4] G. Kaplan, O.Y. Bayraktar, A. Gholampour, O. Gencel, F. Koksal, and T. Ozbakkaloglu, "Mechanical and durability properties of steel fiber-reinforced concrete containing coarse recycled concrete aggregate", *Struct. Concr.,* vol. 22, no. 5, pp. 2791-2812, 2021. [http://dx.doi.org/10.1002/suco.202100028]

[5] X. Zhang, Z. Tang, G. Ke, and W. Li, "Mechanical properties and durability of sustainable concrete containing various industrial solid wastes", *Transp. Res. Rec.,* vol. 2675, no. 12, pp. 797-810, 2021. [http://dx.doi.org/10.1177/03611981211031236]

[6] N. Gupta, R. Siddique, and R. Belarbi, "Sustainable and greener self-compacting concrete incorporating industrial by-products: A review", *J. Clean. Prod.,* vol. 284, p. 124803, 2021. [http://dx.doi.org/10.1016/j.jclepro.2020.124803]

[7] E. Yooprasertchai, A. Khursheed, M.I. Qureshi, A. Ejaz, Q. Hussain, A. Jirasakjamroonsri, and P. Saingam, "Sustainable development of concrete through treated and untreated plastic waste aggregates", *Sci. Rep.,* vol. 14, no. 1, p. 22051, 2024. [http://dx.doi.org/10.1038/s41598-024-73236-8] [PMID: 39333656]

[8] M.H. Lai, J. Zou, B. Yao, J.C.M. Ho, X. Zhuang, and Q. Wang, "Improving mechanical behavior and microstructure of concrete by using BOF steel slag aggregate", *Constr. Build. Mater.,* vol. 277, p. 122269, 2021. [http://dx.doi.org/10.1016/j.conbuildmat.2021.122269]

[9] Z.U. Islam, S. Farooq, O. Wali, F. Ullah, M. Ahmad, and A. Khan, "Enhancing concrete properties through the utilization of steel slag as aggregate replacement", *J. Build. Pathol. Rehabil.,* vol. 10, no. 2, p. 135, 2025. [http://dx.doi.org/10.1007/s41024-025-00653-1]

[10] Z. Chen, L. Huang, L. Yan, H. Cai, X. Luo, and Y. Li, "Autoclaved steel slag coarse aggregate: A potential solution for sustainable concrete production", *Constr. Build. Mater.,* vol. 400, p. 132627, 2023. [http://dx.doi.org/10.1016/j.conbuildmat.2023.132627]

[11] I.K. Ibrahim, M. Rady, N.M. Tawfik, M. Kassem, and S.Y. Mahfouz, "Enhancing strength and sustainability of concrete with steel slag aggregate", *Sci. Rep.,* vol. 15, no. 1, p. 17068, 2025. [http://dx.doi.org/10.1038/s41598-025-01296-5] [PMID: 40379719]

[12] M.E. Mitwally, A. Elnemr, A. Shash, and A. Babiker, "Utilization of steel slag as partial replacement for coarse aggregate in concrete", *Innov. Infrastruct. Solut.,* vol. 9, no. 5, p. 175, 2024. [http://dx.doi.org/10.1007/s41062-024-01464-y]

[13] N.R. Mohanta, and M. Murmu, "A review on the utilization of steel slag as alternative coarse aggregate in concrete: Transforming waste into wealth", *Civ. Eng.,* vol. 50, no. 3, pp. 2269-2304, 2026. [http://dx.doi.org/10.1007/s40996-025-01981-5]

[14] Z. Li, A. Shen, X. Yang, Y. Guo, and Y. Liu, "A review of steel slag as a substitute for natural aggregate applied to cement concrete", *Road Mater. Pavement Des.,* vol. 24, no. 2, pp. 537-559, 2023. [http://dx.doi.org/10.1080/14680629.2021.2024241]

[15] X. Wei, X. Sun, H. Du, W. Ni, X. Kong, and C. Ren, "Recycle of steel slag as cementitious material and fine aggregate in concrete: Mechanical, durability property and environmental impact", *Environ. Sci. Pollut. Res. Int.,* vol. 31, no. 44, pp. 56194-56209, 2024. [http://dx.doi.org/10.1007/s11356-024-34746-0] [PMID: 39261404]

[16] A. Chandra Pal, M. Panda, and P.K. Bhuyan, "A comprehensive study on sustainable development of pavement quality concrete utilising fly-ash and copper slag", *Eur. J. Environ. Civ. Eng.,* vol. 29, no. 9, pp. 1743-1768, 2025. [http://dx.doi.org/10.1080/19648189.2025.2453016]

[17] S. Dutta, and N. Singh, "A brief review on workability characteristics of iron slag concrete", *Mater. Today Proc.,* vol. 82, pp. 408-413, 2023. [http://dx.doi.org/10.1016/j.matpr.2023.04.042]

[18] M.F. Akhtar, A. Faraz, and A. Khitab, "Transforming concrete with steel slag: Exploring the pores' dual effect for sustainable and high−performance urban construction", *Discov. Civ. Eng.,* vol. 2, no. 1, p. 81, 2025. [http://dx.doi.org/10.1007/s44290-025-00243-7]

[19] P. Vu Hong Son, N. Van Nam, N.P. Tran, L. Le-Hoai, and T.D. Ngo, "Steel slag aggregate low-cement concrete: Engineering performance, microstructure and sustainability", *Constr. Build. Mater.,* vol. 436, p. 136827, 2024. [http://dx.doi.org/10.1016/j.conbuildmat.2024.136827]

[20] A. Özcan, and M.B. Karakoç, "The resistance of blast furnace slag- and ferrochrome slag-based geopolymer concrete against acid attack", *Int. J. Civ. Eng.,* vol. 17, no. 10, pp. 1571-1583, 2019. [http://dx.doi.org/10.1007/s40999-019-00425-2]

[21] J. Hu, "Comparison between the effects of superfine steel slag and superfine phosphorus slag on the long-term performances and durability of concrete", *J. Therm. Anal. Calorim.,* vol. 128, no. 3, pp. 1251-1263, 2017. [http://dx.doi.org/10.1007/s10973-017-6107-9]

[22] Y. Li, F. Liu, F. Yu, and T. Du, "A review of the application of steel slag in concrete", *Structures,* vol. 63, p. 106352, 2024. [http://dx.doi.org/10.1016/j.istruc.2024.106352]

[23] R. Gopalakrishnan, and S. Nithiyanantham, "Microstructural, mechanical, and electrical properties of copper slag admixtured cement mortar", *J. Build. Eng.,* vol. 31, p. 101375, 2020. [http://dx.doi.org/10.1016/j.jobe.2020.101375]

[24] A. Chadee, D. Maharaj, Y. Rajapakse, E. Rajack, S. Mendis, H.M. Azamathulla, D.J. Mehta, and U. Rathnayake, "Sustainable use of electric arc furnace slag as a fine aggregate replacement for concrete", *J. Sustain. Res.,* vol. 7, no. 1, p. e250012, 2025. [http://dx.doi.org/10.20900/jsr20250012]

[25] Q. Van Ho, and T.P. Huynh, "A comprehensive investigation on the impacts of steel slag aggregate on characteristics of high-performance concrete incorporating industrial by-products", *J. Build. Eng.,* vol. 80, p. 107982, 2023. [http://dx.doi.org/10.1016/j.jobe.2023.107982]

[26] B.M.A. Herki, A.I. Ali, Y.S. Smail, and K.M. Omer, "An innovative approach to enhancing concrete sustainability: Utilising unprocessed steel slag with low CaO and high SiO2 content", *Buildings,* vol. 15, no. 9, p. 1514, 2025. [http://dx.doi.org/10.3390/buildings15091514]

[27] T.A. Abdalla, and T.S. Alahmari, "Mechanical strength and microstructure properties of concrete incorporating copper slag as fine aggregate: A State-of-the-Art review", *Adv. Civ. Eng.,* vol. 2024, no. 1, p. 4389616, 2024. [http://dx.doi.org/10.1155/2024/4389616]

[28] A. Torres, L. Bartlett, and C. Pilgrim, "Effect of foundry waste on the mechanical properties of Portland cement concrete", *Constr. Build. Mater.,* vol. 135, pp. 674-681, 2017. [http://dx.doi.org/10.1016/j.conbuildmat.2017.01.028]

[29] P. Singh, A.B.D. Roy, and H. Singh, "Mechanical and durability properties of concrete incorporating weathered coarse Linz-Donawitz (LD) steel slag", *J. Build. Eng.,* vol. 61, p. 105301, 2022. [http://dx.doi.org/10.1016/j.jobe.2022.105301]

[30] S. Choudhary, P. Ravi Kishore, and S. Pachaiappan, "Sustainable utilization of waste slag aggregates as replacement of coarse aggregates in concrete", *Mater. Today Proc.,* vol. 59, pp. 240-247, 2022. [http://dx.doi.org/10.1016/j.matpr.2021.11.103]

[31] *IS 8112: Specification for 43 Grade Ordinary Portland Cement,* Bureau of Indian Standards (BIS): New Delhi, India, 2013. Available from: https://archive.org/details/gov.in.is.8112.2013

[32] *IS 383: Coarse and Fine Aggregate for Concrete - Specification,* Bureau of Indian Standards (BIS): New Delhi, India, 2016. Available from: https://archive.org/details/gov.in.is.383.2016/is.383.2016/

[33] *IS 1199 Part 2 : Fresh Concrete - Methods of Sampling and Testing - Part 2: Determination of Slump,* Bureau of Indian Standards (BIS): New Delhi, India, 2018. Available from: https://infralens.in/code/IS-1199-Part-2-2018

[34] *IS 516 : Part 1 : Sec 1 : 2021: Hardened concrete methods of test part 1 testing of strength of hardened concrete section 1 compressive,flexucal and split tensile strength (First Revision),* Bureau of Indian Standards (BIS): New Delhi, India, 2021. Available from: https://archive.org/details/gov.in.is.516.1.1.2021

[35] *ASTM C597-22: Standard Test Method for Ultrasonic Pulse Velocity Through Concrete,* ASTM International: West Conshohocken, PA, USA, 2022. Available from: https://webstore.ansi.org/standards/astm/astmc59722red?ad_acct=0000&gad_source=1&gad_campaignid=22318459439&gclid=EAIaIQobChMIjfijoOHglgMVnJKDBx1bbC3REAAYAyAAEgKkb_D_BwE

[36] *IS 1237 : Cement Concrete Flooring Tiles - Specification*, Bureau of Indian Standards (BIS): New Delhi, India, 2012. Available from: https://archive.org/details/gov.in.is.1237.2012/is.1237.2012/

[37] *ASTM C642-21: Standard Test Method for Density, Absorption, and Voids in Hardened Concrete*, ASTM International: West Conshohocken, PA, USA, 2021. Available from: https://store.astm.org/c0642-21.html

[38] *DIN 1048-5, Testing Concrete—Testing of Hardened Concrete (Permeability of Water)*, Beuth Verlag: Berlin, Germany, 1991. Available from: https://www.scribd.com/document/188461778/DIN-1048

[39] *ASTM C267-20: Standard Test Methods for Chemical Resistance of Mortars, Grouts, and Monolithic Surfacings and Polymer Concretes*, ASTM International: West Conshohocken, PA, USA, 2020. Available from: https://webstore.ansi.org/standards/astm/astmc26720red?srsltid=AfmBOoooOYxTCRkcPWOmOjojlW-soKd33ckDXG31Ic7DL3ADKtrf47RD

[40] V. Baroghel-Bouny, P. Belin, M. Maultzsch, and D. Henry, "AgNO3 spray tests: Advantages, weaknesses, and various applications to quantify chloride ingress into concrete. Part 1: Non-steady-state diffusion tests and exposure to natural conditions", *Mater. Struct.*, vol. 40, no. 8, pp. 759-781, 2007. [http://dx.doi.org/10.1617/s11527-007-9233-1]

[41] D.Y. Yoo, N. Banthia, and Y.S. Yoon, "Predicting the flexural behavior of ultra-high-performance fiber-reinforced concrete", *Cement Concr. Compos.*, vol. 74, pp. 71-87, 2016. [http://dx.doi.org/10.1016/j.cemconcomp.2016.09.005]

[42] "ACI PRC-544.1R-96: Report on fiber reinforced concrete (Reapproved 2023)", Available from: https://www.concrete.org/store/productdetail.aspx?ItemID=544196&Format=DOWNLOAD&Language=English&Units=US_AND_METRIC

[43] V. Afroughsabet, and T. Ozbakkaloglu, "Mechanical and durability properties of high-strength concrete containing steel and polypropylene fibers", *Constr. Build. Mater.*, vol. 94, pp. 73-82, 2015. [http://dx.doi.org/10.1016/j.conbuildmat.2015.06.051]

[44] M. Mastali, and A. Dalvand, "Use of silica fume and recycled steel fibers in Self-Compacting Concrete (SCC)", *Constr. Build. Mater.*, vol. 125, pp. 196-209, 2016. [http://dx.doi.org/10.1016/j.conbuildmat.2016.08.046]

[45] Y. Zheng, X. Wu, G. He, Q. Shang, J. Xu, and Y. Sun, "Mechanical properties of steel fiber-reinforced concrete by vibratory mixing technology", *Adv Civ Eng*, p. 9025715, 2018. [http://dx.doi.org/10.1155/2018/9025715]

[46] Ş. Yazıcı, G. İnan, and V. Tabak, "Effect of aspect ratio and volume fraction of steel fiber on the mechanical properties of SFRC", *Constr. Build. Mater.*, vol. 21, no. 6, pp. 1250-1253, 2007. [http://dx.doi.org/10.1016/j.conbuildmat.2006.05.025]

[47] J. Ahmad, Z. Zhou, and A.F. Deifalla, "Steel fiber reinforced self-compacting concrete: A comprehensive review", *Int. J. Concr. Struct. Mater.*, vol. 17, no. 1, p. 51, 2023. [http://dx.doi.org/10.1186/s40069-023-00602-7]

[48] H.J. Qureshi, S.A. Alghamdi, A. Majdi, J. Ahmad, C. Rahmawati, W. Alattyih, and A. Alzlfawi, "Utilization of steel slag in concrete: A review on durability and microstructure analysis", *Rev. Adv. Mater. Sci.*, vol. 64, no. 1, p. 20250086, 2025. [http://dx.doi.org/10.1515/rams-2025-0086]